Walter A. Rosenblith New Investigator Award
RESEARCH REPORT

HEALTH EFFECTS INSTITUTE

Number 201
July 2020

Understanding the Functional Impact of VOC–Ozone Mixtures on the Chemistry of RNA in Epithelial Lung Cells

Lydia M. Contreras, Juan C. Gonzalez-Rivera, Kevin C. Baldridge, Dongyu S. Wang, Jamie C. L. Chuvalo-Abraham, and Lea Hildebrandt Ruiz

ISSN 1041-5505 (print)
ISSN 2688-6855 (online)

Understanding the Functional Impact of VOC–Ozone Mixtures on the Chemistry of RNA in Epithelial Lung Cells

Lydia M. Contreras, Juan C. Gonzalez-Rivera, Kevin C. Baldridge, Dongyu S. Wang, Jamie C. L. Chuvalo-Abraham, and Lea Hildebrandt Ruiz

with a Critique by the HEI Review Committee

Research Report 201

Health Effects Institute

Boston, Massachusetts

Trusted Science • Cleaner Air • Better Health

Publishing history: This document was posted at *www.healtheffects.org* in July 2020.

Citation for document:

Contreras LM, Gonzalez-Rivera JC, Baldridge KC, Wang DS, Chuvalo-Abraham JCL, Ruiz LH. 2020. Understanding the Functional Impact of VOC–Ozone Mixtures on the Chemistry of RNA in Epithelial Lung Cells. Research Report 201. Boston, MA:Health Effects Institute.

 Cameographics, Belfast, Me., Compositor. Printed by Recycled Paper Printing, Waltham, Mass. Library of Congress Catalog Number for the HEI Report Series: WA 754 R432.

Cover paper: made with at least 55% recycled content, of which at least 30% is post-consumer waste; free of acid and elemental chlorine. Text paper: made with 100% post-consumer waste recycled content; acid free; no chlorine used in processing. The book is of permanent archival quality.

CONTENTS

ABOUT HEI

The Health Effects Institute is a nonprofit corporation chartered in 1980 as an independent research organization to provide high-quality, impartial, and relevant science on the effects of air pollution on health. To accomplish its mission, the institute

- Identifies the highest-priority areas for health effects research;
- Competitively funds and oversees research projects;
- Provides intensive independent review of HEI-supported studies and related research;
- Integrates HEI's research results with those of other institutions into broader evaluations; and
- Communicates the results of HEI's research and analyses to public and private decision makers.

HEI typically receives balanced funding from the U.S. Environmental Protection Agency and the worldwide motor vehicle industry. Frequently, other public and private organizations in the United States and around the world also support major projects or research programs. HEI has funded more than 340 research projects in North America, Europe, Asia, and Latin America, the results of which have informed decisions regarding carbon monoxide, air toxics, nitrogen oxides, diesel exhaust, ozone, particulate matter, and other pollutants. These results have appeared in more than 260 comprehensive reports published by HEI, as well as in more than 2,500 articles in the peer-reviewed literature.

HEI's independent Board of Directors consists of leaders in science and policy who are committed to fostering the public–private partnership that is central to the organization. The Research Committee solicits input from HEI sponsors and other stakeholders and works with scientific staff to develop a Five-Year Strategic Plan, select research projects for funding, and oversee their conduct. The Review Committee, which has no role in selecting or overseeing studies, works with staff to evaluate and interpret the results of funded studies and related research.

All project results and accompanying comments by the Review Committee are widely disseminated through HEI's website (*www.healtheffects.org*), printed reports, newsletters and other publications, annual conferences, and presentations to legislative bodies and public agencies.

ABOUT THIS REPORT

Research Report 201, *Understanding the Functional Impact of VOC–Ozone Mixtures on the Chemistry of RNA in Epithelial Lung Cells,* presents a research project funded by the Health Effects Institute and conducted Dr. Lydia M. Contreras of the University of Texas, Austin, and her colleagues. This research was funded under HEI's Walter A. Rosenblith New Investigator Award Program, which provides support to promising scientists in the early stages of their careers. The report contains three main sections.

The HEI Statement, prepared by staff at HEI, is a brief, nontechnical summary of the study and its findings; it also briefly describes the Review Committee's comments on the study.

The Investigators' Report, prepared by Contreras and colleagues, describes the scientific background, aims, methods, results, and conclusions of the study.

The Critique, prepared by members of the Review Committee with the assistance of HEI staff, places the study in a broader scientific context, points out its strengths and limitations, and discusses remaining uncertainties and implications of the study's findings for public health and future research.

This report has gone through HEI's rigorous review process. When an HEI-funded study is completed, the investigators submit a draft final report presenting the background and results of the study. This draft report is first examined by outside technical reviewers and a biostatistician. The report and the reviewers' comments are then evaluated by members of the Review Committee, an independent panel of distinguished scientists who have no involvement in selecting or overseeing HEI studies. During the review process, the investigators have an opportunity to exchange comments with the Review Committee and, as necessary, to revise their report. The Critique reflects the information provided in the final version of the report.

HEI STATEMENT

Synopsis of Research Report 201

Effects of a VOC–Ozone Mixture on Human Lung Epithelial Cells

BACKGROUND

In this study, Dr. Lydia Contreras, a recipient of HEI's 2014 Walter A. Rosenblith New Investigator Award, and her colleagues evaluated how exposure to components of air pollution affected the oxidation of ribonucleic acid (RNA) inside lung cells. The role of RNA oxidation in cellular responses is drawing increased attention, because several species of RNA — including messenger, transfer, and micro RNA — play key roles inside cells, particularly in the regulation of protein synthesis. The investigators also studied how the oxidation of RNA might affect pathways inside the cell.

APPROACH

The investigators mixed 790 ppb acrolein, 670 ppb methacrolein, and 4 ppm ozone in a dark chamber at 37°C. After 10 minutes, the aged VOC–ozone mixture was introduced into a module containing the human lung epithelial cell line BEAS-2B in an air–liquid interface system, in which the gases were passed over the top surface of the cells grown on a membrane inserted in a cell culture plate. Exposures lasted 90 minutes. The investigators monitored the composition of gas-phase compounds as well as particle size distribution and particle chemical composition.

Contreras and colleagues identified specific RNA transcripts that were either up- or downregulated by the exposures. They also identified specific transcripts that were oxidized by the exposure by using an antibody specific to a particularly sensitive RNA oxidation product, 8-oxo-7,8-dihydroguanine (8-oxoG).

Using this information, the investigators performed analyses to identify the biological pathways inside the cells that were most associated with these changes in transcription. Having identified specific pathways, they then performed biological assays to see whether the oxidation of transcripts also had effects on levels of specific proteins or lipids in the exposed cells. Based on preliminary data suggesting that genes involved in the cytoskeleton structure were both oxidized and downregulated by the VOC–ozone exposure, they used microscopy to evaluate effects on the actin cytoskeleton. They also evaluated markers of cell injury and death — lactate dehydrogenase (LDH) and adherence to the culture plate.

MAIN RESULTS AND INTERPRETATION

Exposure to the VOC–ozone mixture for 90 minutes resulted in 153 upregulated transcripts, 113 downregulated transcripts, and 222 8-oxo-G-enriched transcripts that were preferentially oxidized in the

What This Study Adds

- The study evaluated how exposure of lung cells to volatile organic compounds (VOCs) plus ozone affects oxidation of ribonucleic acid (RNA), a key component of cells.
- VOC–ozone exposure resulted in multiple oxidized transcripts, as well as up- or downregulated transcripts. Pathways associated with the oxidation of specific transcripts included cholesterol synthesis and organization of the cell's structure (the cytoskeleton).
- However, VOC–ozone exposure also increased markers of cell injury and death, so questions remain about the potential cytotoxicity of the VOC–ozone mixture used. Nonetheless, this approach provides a powerful and logical template for future research on the effects of air pollution on RNA oxidation.

This Statement, prepared by the Health Effects Institute, summarizes a research project funded by HEI and conducted by Dr. Lydia M. Contreras at the University of Texas, Austin, and colleagues. Research Report 201 contains both the detailed Investigators' Report and a Critique of the study prepared by the Institute's Review Committee.

VOC–ozone exposed cells (see Statement Figure). Eight transcripts were in the overlapping set of oxidized and downregulated transcripts. One of the eight was farnesyl diphosphate farnesyltransferase 1, an enzyme involved in cholesterol biosynthesis.

Preliminary analysis of the cellular pathways suggested that oxidation was associated with changes in the cytoskeleton, which was confirmed by microscopy analysis of the organization of the cytoskeleton. However, the VOC–ozone mixture also increased markers of cell injury and death: there were large increases in LDH concentrations and loss of adherence to the culture membrane, suggesting that exposure to the VOC–ozone mixture was cytotoxic.

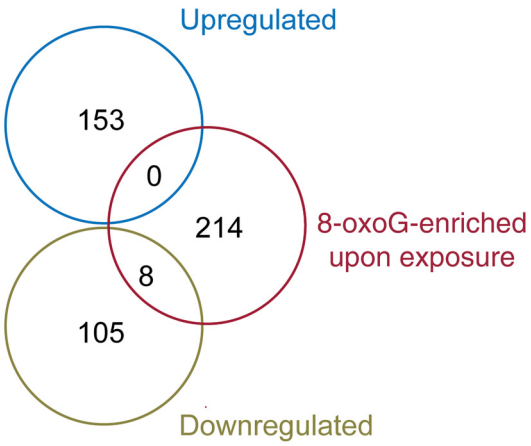

Statement Figure. Number of upregulated, downregulated, and 8-oxoG-enriched transcripts after exposure of lung epithelial cells to a VOC–ozone mixture.

REVIEW OF THE REPORT

In its independent review, the HEI Review Committee considered the study to be an exciting new approach to the toxicology of air pollution and an important initial attempt to understand an understudied area: the role of messenger RNA regulation, modification, and oxidation in the effects of exposure to air pollutants. The investigators used a logical combination of powerful approaches — including transcriptome analysis, biochemistry, and cell biology — to identify candidate genes and pathways for further evaluation of the effects of exposure to pollutants.

Exposing cells to a mixture of gases — ozone plus the VOCs acrolein and methacrolein — was potentially relevant to assessing the effects of reactants that may be found in some urban atmospheres. The exposure generation and physicochemical characterization were state of the art. The air–liquid interface in vitro system was more physiologically representative than many in vitro methods because cells are directly exposed to the pollutant gas mixture instead of mixing pollutants into the culture medium.

However, the Committee noted several important limitations in the study design that reduced confidence in the generalizability of the results toward understanding the role of RNA oxidation after exposure to air pollution. One major limitation was that the concentrations of VOCs and ozone used were much higher than would be found even in heavily polluted urban environments and appeared to be cytotoxic. Also, the results were based on exposure of cells to a single mixture, at one high exposure level, and measured at only one timepoint. In addition, the study focused on a single RNA oxidation product, 8-oxoG. This focus was understandable given the availability of a specific monoclonal antibody that recognized this molecule but was not well justified from a theoretical perspective. In future studies, other potentially more biologically relevant RNA oxidation products need to be identified using more sensitive techniques.

Nonetheless, the Committee considered the study to be an important preliminary demonstration of RNA oxidation in lung cells exposed to a VOC–ozone mixture. This powerful combination of techniques — including transcriptome analysis, biochemistry, and cell biology — offers a template to be applied to more exact and comprehensive studies in the future.

Understanding the Functional Impact of VOC–Ozone Mixtures on the Chemistry of RNA in Epithelial Lung Cells

Lydia M. Contreras[1], Juan C. Gonzalez-Rivera[1], Kevin C. Baldridge[1], Dongyu S. Wang[1], Jamie C. L. Chuvalo-Abraham[1], and Lea Hildebrandt Ruiz[1]

[1]*McKetta Department of Chemical Engineering, University of Texas, Austin*

ABSTRACT

Introduction Ambient air pollution is associated with premature death caused by heart disease, stroke, chronic obstructive pulmonary disease (COPD*), and lung cancer. Recent studies have suggested that ribonucleic acid (RNA) oxidation is a sensitive environment-related biomarker that is implicated in pathogenesis.

Aims and Methods We used a novel approach that integrated RNA-Seq analysis with detection by immunoprecipitation techniques of the prominent RNA oxidative modification 8-oxo-7,8-dihydroguanine (8-oxoG). Our goal was to uncover specific messenger RNA (mRNA) oxidation induced by mixtures of volatile organic compounds (VOCs) and ozone in healthy human epithelial lung cells. To this end, we exposed the BEAS-2B human epithelial lung cell line to the gas- and particle-phase products formed from reactions of 790 ppb acrolein (ACR) and 670 ppb methacrolein (MACR) with 4 ppm ozone.

Results Using this approach, we identified 222 potential direct targets of oxidation belonging to previously described pathways, as well as uncharacterized pathways, after air pollution exposures. We demonstrated the effect of our VOC–ozone mixtures on the morphology and actin cytoskeleton of lung cells, suggesting the influence of selective mRNA oxidation in members of pathways regulating physical components of the cells. In addition, we observed the influence of the VOC–ozone mixtures on metabolic cholesterol synthesis, likely implicated as a result of the incidence of mRNA oxidation and the deregulation of protein levels of squalene synthase (farnesyl-diphosphate farnesyltransferase 1 [FDFT1]), a key enzyme in endogenous cholesterol biosynthesis.

Conclusions Overall, our findings indicate that air pollution influences the accumulation of 8-oxoG in transcripts of epithelial lung cells that largely belong to stress-induced signaling and metabolic and structural pathways. A strength of the study was that it combined traditional transcriptome analysis with transcriptome-wide 8-oxoG mapping to facilitate the discovery of underlying processes not characterized by earlier approaches. Investigation of the processes mediated by air pollution oxidation of RNA molecules in primary cells and animal models needs to be explored in future studies. Our research has thus opened new avenues to further inform the relationship between atmospheric agents on the one hand and cellular responses on the other that are implicated in diseases.

INTRODUCTION

Levels of air pollution continue to rise to alarming heights in many cities around the globe, and almost the entire global population is exposed to detectable levels of pollution. Ambient air pollution is estimated to cause more than 4.2 million premature deaths per year, largely from heart disease, stroke, COPD, and lung cancer (WHO

This Investigators' Report is one part of Health Effects Institute Research Report 201, which also includes a Critique by the Review Committee and an HEI Statement about the research project. Correspondence concerning the Investigators' Report may be addressed to Dr. Lydia M. Contreras, McKetta Department of Chemical Engineering, University of Texas at Austin, Department of Statistics & Data Sciences, Patterson Hall 141MC & GDC 7.510, Austin, TX 78712; e-mail: *lcontrer@che.utexas.edu*.

Although this document was produced with partial funding by the United States Environmental Protection Agency under Assistance Award CR–83467701 to the Health Effects Institute, it has not been subjected to the Agency's peer and administrative review and therefore may not necessarily reflect the views of the Agency, and no official endorsement by it should be inferred. The contents of this document also have not been reviewed by private party institutions, including those that support the Health Effects Institute; therefore, it may not reflect the views or policies of these parties, and no endorsement by them should be inferred.

* A list of abbreviations and other terms appears at the end of this volume.

2018). Urban atmospheres consist of complex, heterogeneous mixtures of reactive gas substances and small particles directly emitted by motor vehicles, industry, and other sources or formed over time in the atmosphere. Major components of these atmospheres, such as ozone, particulate matter (PM), and VOCs, have the potential to cause harmful effects on health. Ozone, for instance, is associated with a risk of cardiovascular and respiratory diseases by way of inflammatory responses in sensory nerves and injury in lungs (Graham et al. 2001). PM $\leq$2.5 μm in aerodynamic diameter ($PM_{2.5}$) contributes to a decline in lung, heart, and brain activity through the deposition and toxic action of particles and to deterioration in immune responses (Cohen et al. 2017). In addition, VOCs such as ACR and MACR, which can react with ozone to generate more particles, induce respiratory, gastrointestinal, and cardiovascular irritation by activation of signaling factors in sensory processes (Faroon et al. 2008).

From the cellular perspective, air pollution has been shown to exert stress responses characterized by signaling, metabolic, and morphological alterations. As such, exposure to ozone triggers production of pro-inflammatory and signaling cytokines, such as interleukins IL-1β, IL-6, and IL-8 and tumor necrosis factor-alpha, that can regulate mechanisms of adaptation, proliferation, and apoptosis (Cho et al. 2007; Doyle et al. 2007). Exposure to ACR results in interaction with membrane receptors, such as the epithelial growth factor receptor (EGFR) and the transient receptor potential cation channel, and activation of nuclear factor kappa B, a transcription factor that can mediate responses such as cell proliferation and apoptosis (Kehrer and Biswal 2000; Takeuchi et al. 2001). Given its amphiphilic character, ACR has also been reported to alter lipid metabolic processes, increasing phospholipid and triglyceride levels (Henning et al. 2017). However, the underlying mechanisms that lead to these alterations are not well understood.

Numerous studies are moving toward novel biomolecular approaches to explore RNA chemistry, function, and expression in order to characterize cellular responses to environmental factors. One of the most interesting approaches has been the use of the RNA oxidative modification 8-oxoG as a sensitive biomarker of environmental exposures (Baldridge et al. 2015). This adduct has been successfully evaluated in epidemiological and cell culture exposures (Andreoli et al. 2015; Baldridge et al. 2015). In addition, transcriptome-wide analysis of chemical exposures, or toxicogenomic analysis, has been used to evaluate global alterations in mRNA expression, providing insights into the genes and physiological pathways affected by air pollution exposures (McHale et al. 2010).

In the current study, we combined transcriptome-wide analysis with detection of 8-oxoG by immunoprecipitation techniques to uncover specific transcript oxidation induced by VOC–ozone mixtures to elucidate key cellular pathways modified by RNA oxidation; the mixtures used were derived from 790 ppb ACR, 670 ppb MACR, and 4 ppm ozone. We adapted the N6-methyladenosine sequencing approach based on immunocapturing and high-throughput sequencing for identification of 8-oxoG–containing mRNA (Dominissini et al. 2013). Our study was performed in BEAS-2B cells, a well-established model for epithelial lung cells air toxicity studies, exposed to an acute dose of gas and particle pollutants in an air–liquid interface (ALI) exposure system. We showed that the use of 8-oxoG RNA-Seq is a relevant tool for air toxicology; to our knowledge, ours is the first study to use this approach to characterize the cellular effects resulting from air pollution exposures. We identified 222 potential direct targets of oxidation that belong to previously proposed pathways, as well as uncharacterized pathways, on air pollution exposures. An important aspect of our study was to develop a novel molecular model of air toxicity that would allow us to demonstrate that specific oxidation of RNA can influence stress-related signaling pathways and alterations in metabolic pathways and can lead to morphological changes in lung cells.

BACKGROUND

HEALTH EFFECTS OF OZONE AND ACROLEIN

Ozone is a major product of photochemical reactions that can induce formation of reactive oxygen species (ROS), leading to oxidative stress. Studies of ozone health effects have suggested that it can generate oxidative injury in lung and brain tissue. The respiratory tract is most likely the first organ affected by ozone exposure, causing impairment of pulmonary function and reduction of airway antioxidant defenses (Sousa et al. 2013). In addition, studies have demonstrated that ozone can produce functional changes associated with neurodegenerative diseases. For instance, the striatum and substantia nigra are affected after 30 days of exposure to 0.25 ppm ozone (Dorado-Martinez et al. 2001). Specifically, ozone can alter redox signals that contribute to the activation of dopaminergic neuronal death (Rivas-Arancibia et al. 2010).

ACR and MACR are highly reactive unsaturated aldehydes released into the atmosphere during combustion of petrochemical products and burning of wood and cigarettes (Moghe et al. 2015). They are also initial major photochemical products of principal VOCs such as

1,3-butadiene and isoprene. Given that ACR can exert adverse effects on diverse cellular pathways and organs, ACR exposures have been associated with a wide range of health conditions, including cardiovascular, respiratory, neuronal, and metabolic diseases. When inhaled, ACR can cause irritation of the upper respiratory system and can trigger airway sensory receptors that mediate bronchoconstriction (Henning et al. 2017). Furthermore, it can cause apnea, shortness of breath, cough, airway obstruction, and mucous infection (Henning et al. 2017). ACR can cross the alveolar–capillary membrane and hence is thought to contribute to cardiovascular injury. Specifically, it can interact with cation channel receptors, triggering the opening of channels that allow neuronal activation of pain signaling and can increase local tissue inflammation, blood flow and vascular permittivity, and edema (Conklin 2016). Because of its amphiphilic nature, ACR can alter lipid metabolism and so is linked to dyslipidemia and atherogenesis. For instance, ACR in doses of 0.1 to 0.5 mg/kg in mice induces higher levels of very-low-density lipoprotein, phospholipids, and triglycerides (Conklin et al. 2010). ACR can also generate adducts with high-density lipoprotein, impairing the transport of cholesterol from peripheral tissues to the liver, and hence inducing accumulation of cholesterol that likely leads to atherogenesis (Chadwick et al. 2015).

MOLECULAR EFFECTS OF AIR POLLUTION ON CELLULAR COMPONENTS

Detection of stress-induced modifications occurring in cellular components such as lipids, proteins, and DNA is widely used to characterize cytotoxic effects of air pollution. These markers can be influenced by environmental factors, and hence they constitute robust markers of exposure. Components of the cell and subcellular membranes, such as polyunsaturated fatty acids, are highly susceptible to oxidation (Barrera 2012). The end products of this process consist of aldehydes and polymerized carbonyl compounds that can cause a decrease in membrane fluidity, inactivation of membrane-bound proteins and receptors, and changes in permeability (Moghe et al. 2015). These events are key contributors to epithelial-to-mesenchymal transition, cell fibrosis, and the progression of several cardiovascular diseases (Barker et al. 2014). As such, the incidence of lipid oxidation has become remarkably effective as a clinical biomarker in multiple environmental assessments; chronic and acute doses of ozone, for instance, induce higher levels of lipid peroxidation markers in healthy young adults with broad ranges of ambient ozone exposure (Chen et al. 2007). Multiple products of lipid peroxidation, such as malondialdehyde and 4-hydroxynonenal, can induce further damage in DNA and proteins (Castro et al. 2017; Del Rio et al. 2005). In proteins, oxidative species can post-translationally modify amino acids, resulting in several modified products such as alkoxy, peroxide, hydroxy, and carbonyl groups (Davies 2016). These modifications lead to fragmentation, aggregation, and protein unfolding, contributing to protein inactivation (Davies 2016). As such, ozone causes protein oxidation in rats at doses of 0.25 ppm for 4 hours (Rivas-Arancibia et al. 2015) and, during in vitro studies, at levels of 50 and 200 ppb ozone, suggesting formation of protein aggregates attributable to the cross-linking capacity of ozone (Kampf et al. 2015). Furthermore, direct exposures of rats to ACR, in concentrations of 9.2 mg/kg, can induce ACR–protein adducts (Li et al. 2004). Although cells can detoxify some of these adducts by reducing radical groups and by lysosomal and proteasomal proteolysis, certain oxidized proteins are poorly handled, causing the accumulation of dysfunctional proteins (Lai et al. 2016). Increased levels of modified proteins have been described in COPD, diabetes, atherosclerosis, and neurodegenerative diseases (Almogbel and Rasheed 2017; Hohn et al. 2013; Lai et al. 2016).

In addition to the interest in protein and lipid modifications, more attention has emerged in elucidating the mutagenic effects of ROS on nucleic acids. Nucleic acids are specifically sensitive to chemical damage, because oxygen and nitrogen atoms in the nucleobases are reactive to a variety of radicals. In DNA, environmental stress can cause strand breaks, DNA and protein crosslinking, and formation of more than 20 oxidized adducts (Cooke et al. 2003). For instance, ACR in concentrations from 25 to 100 μM has been shown to cause DNA strand breaks and an increase in formation of nucleic acid oxidation (Li et al. 2008). Similarly, 60 to 120 ppb of ozone exposure has been shown to induce DNA backbone cleavage and formation of RNA base oxidation in airway cells (Cheng et al. 2003). Among the canonical nucleobases, oxidation occurs preferentially at a guanine base, resulting in the formation of 8-oxoG. This modification has been the most notable base oxidation in RNA with respect to alterations in genetic information (Dai et al. 2018). Interestingly, under normal physiological conditions and under stress conditions, RNA oxidation is more predominant than DNA oxidation, suggesting that RNA is more susceptible than DNA to forming oxidation products (Li et al. 2014). This phenomenon appears to be determined by differences in structure, packaging, repair, and localization (Simms and Zaher 2016). RNA oxidation has generated wide interest, given that certain mRNAs and non-coding RNAs are more prone to oxidation than others (Shan and Lin 2006; Wang et al. 2015). Indeed, the mechanism of RNA oxidation appears to be highly selective, because several abundant transcripts are less oxidized

than certain scarce transcripts (Shan et al. 2003). This process has functional repercussions on RNA, because oxidation facilitates noncanonical base pairing, altering the native structure and protein recognition (Simms and Zaher 2016). Some modifications can interfere with and even prevent the decoding process on the ribosome, affecting translation fidelity and efficiency and scaling the detrimental effects of RNA oxidation by inducing reductions in protein levels and protein misfolding (Calabretta et al. 2015). Interestingly, accumulation of oxidized RNA has been described in neurodegenerative diseases such as Alzheimer's disease, Parkinson's disease, and amyotrophic lateral sclerosis, where protein downregulation and aggregation are hallmarks of these conditions (Nunomura et al. 2012). Our earlier study (Baldridge et al. 2015) using A549 adenocarcinomic human alveolar basal epithelial cells described an increase in RNA oxidation after exposures to mixtures of 872 ppb ACR, 698 ppb MACR, and 4 ppm ozone. Overall, the observations offered here highlight the relevance of RNA oxidation from a systems biology approach, because they make obvious the links between defective molecular functions and cellular networks affected by exposures.

OMICS STUDIES OF THE IMPACT OF AIR POLLUTION

Two major challenges in understanding the toxicological effects of air pollution are to comprehensively characterize the circuitry of responsive pathways and to provide an integrated outlook on the cell physiology from exposure to disease. Advances in omics technologies have increasingly aided progress toward a mechanistic understanding, with a growing number of epidemiological, animal, and cell exposure studies conducting global expression analysis. A summary of current literature is presented in Additional Materials 3: Appendix C, on the HEI website at *www.healtheffects.org/publications*. As such, transcriptomic studies using a variety of atmospheric stresses have found common alterations in pathways implicated in oxidative stress, metabolism of xenobiotics, and inflammatory cytokine responses. In addition, gene expression changes in pathways involved in DNA damage and repair, cell cycle, DNA synthesis, gene transcription, metabolism of lipids and lipoproteins, extracellular matrix remodeling, and cytoskeleton reorganization have been shown to be dependent on the physicochemical attributes of the atmospheric stress and the dose of exposure (magnitude, duration, and recurrence). Although protein levels often do not immediately reflect alterations in the transcriptome, the pathways identified by toxicology proteomic studies clearly overlap with the pathways described by transcriptomics studies. As such, proteomic profiling exhibits stress-induced alterations of many pathways involved in oxidative stress, xenobiotic metabolism, pro-inflammatory cytokines, DNA repair, signal transduction, cell proliferation, transcriptional regulation, cholesterol biosynthesis pathways, and cytoskeleton organization (Additional Materials 3: Appendix C). Protein profiling has also been demonstrated to be valuable in deriving the status of biological mechanisms, because proteins are more proximal to the phenotype. Overall, omics approaches have enabled the direct identification of key mechanisms underlying exposure-related disease as well as the prediction of novel biomarkers of exposure.

SPECIFIC AIMS

The central hypothesis of this study was that pro-oxidant air, represented by VOC–ozone mixtures, induces changes in relevant mRNAs that influence the activity of cellular pathways, ultimately leading to adverse cellular effects.

Specific Aim 1 Our first specific aim was to establish an exposure model to determine the effects of acute doses of VOC–ozone mixtures on the chemical status of all RNAs in lung cells.

Specific Aim 2 Our second specific aim was to determine adverse effects on cells by VOC–ozone mixtures via oxidation of RNA.

METHODS

BEAS-2B CELL CULTURES

BEAS-2B cell cultures (CRL-9609, ATCC, Manassas, VA) were initiated from cryopreserved cells in pre-coated T-75 culture flasks following the supplier's instructions. Cells were cultured in 23 mL of complete bronchial epithelial cell growth medium (BEGM, Lonza, Walkersville, MD), except for GA-1000 (gentamycin–amphotericin B mix), as recommended by ATCC to maintain healthy cells, with a seeding density of 225,000 cells at 37°C under an atmosphere containing 5% CO_2 and in a humidified incubator. Cells were incubated for 4 days until reaching 70%–80% confluence, with medium renewal 48 hours after seeding. The cells were then passaged to collagen-coated inserts (30-mm-diameter hydrophilic PTFE with pore size of 0.4 μm, EMD Millipore, Burlington, MA) housed in 6-well plates (Costar Clear Multiple Well Plates, Corning, NY) with a seeding density of 200,000 cells and incubated for 24 hours with 0.8 mL and 1.1 mL of medium in the apical

and basolateral side, respectively. Cell culture inserts were coated with 1 mL of 57 μg/mL of Bovine Collagen Type I (Advanced BioMatrix, Carlsbad, CA) in BEGM 24 hours before seeding. Two hours before exposure, the medium from the apical cell surface was completely removed, and the medium from the basolateral cell surface was renewed with fresh complete medium. Cell counting was conducted using 0.6 mL of cell suspension in a viability analyzer (Vi-Cell XR, Beckman Coulter, Brea, CA).

AIR POLLUTION GENERATION AND CHARACTERIZATION

VOC precursors and ozone were mixed inside a 10-m^3 Teflon chamber at 1 atmosphere and 37.3°C under high relative humidity (RH > 35%) in the dark to generate gas- and particle-phase pollutants. Before each experiment, the chamber was cleaned by injecting high concentrations of ozone (>1 ppm) to react away residual organics left over from previous experiments. Excess ozone and cleaning products were then removed by flushing the chamber with dried clean air (<10 particles/cm^3 and <5 ppb gas-phase impurities) for at least 12 hours. Afterward, humidified clean air was flushed through the chamber to raise the RH. Each VOC precursor was injected separately by first transferring 24 μL of ACR (90% stabilized, Sigma-Aldrich, St. Louis, MO) or MACR (95% stabilized, Sigma-Aldrich) into a glass gas-sampling tube (250 mL, Kimble-Chase, Vineland, NJ), which was flushed with clean air into the chamber at 2 liters per minute (LPM) for at least 10 minutes, equivalent to ACR and MACR starting concentrations of 790 and 670 ppb, respectively. The ozone used for cleaning and VOC oxidation is produced using an ozone generator (TG-10, Ozone Solutions, Hull, IA) using UHP O_2 via corona discharge. Approximately 4 ppm of initial ozone was injected for each exposure experiment. Once mixed, the ozone, ACR, and MACR concentrations decrease over time as the result of oxidation chemistry.

Particle size distributions were characterized using a scanning electrical mobility spectrometer (SEMS, model 2002, Brechtel, Hayward, CA). The SEMS consisted of a differential mobility analyzer (DMA) and a butanol condensation particle counter. The DMA charges and separates particles based on their electrical mobility, which is a function of the particle diameter. Size-selected particles are counted by the condensation particle counter via light scattering. The SEMS is configured to characterize the distribution of suspended particles using 60 discrete size bins ranging from 10 to 1000 nm in diameter, with sheath and polydisperse flow rates set to 5 and 0.35 LPM. A preimpactor, a Nafion membrane dryer, and a polonium-210 strip neutralizer were used to condition the polydisperse sample flow upstream of the DMA column.

The particle-phase bulk chemical composition was measured using an aerosol chemical speciation monitor (ACSM) (Aerodyne, Billerica, MA). Using electron impact ionization, the ACSM can measure the submicron, nonrefractory aerosol bulk composition at 1-minute intervals (Budisulistiorini et al. 2013; Ng et al. 2011). Using a standard fragmentation table (Allan et al. 2004), an ACSM can speciate the aerosol content into organics, nitrate, sulfate, ammonium, and chloride (Ng et al. 2011). Our ACSM was calibrated with 300-nm size-selected ammonium nitrate and ammonium sulfate aerosols generated from nebulized 0.005-M solutions to determine the necessary ion-to-mass signal conversion factors using default procedures recommended by the instrument manufacturer. ACSM data were analyzed in Igor Pro V6.37 software (Wavemetrics, Portland, OR) using ACSM local v1603 (Aerodyne) and other custom routines. A collection efficiency of 0.5 was assumed for the ACSM; this was consistent with other aerosol mass spectrometers using similar sample-inlet and ion-generation methods (Canagaratna et al. 2007; Ng et al. 2011). Besides ACR, MACR, and ozone, no additional nitrogen oxides, reactive chlorine compounds, or sulfur oxides were introduced into the chamber.

A high-resolution time-of-flight chemical ionization mass spectrometer (CIMS, Aerodyne) was used to monitor the molecular composition of gas-phase compounds using $(H_2O)_{0-2}H_3O^+$ clusters as the chemical ionization reagents (Aljawhary et al. 2013), with $(H_2O)H_3O^+$ being the most abundant reagent ion. The chemical ionization used in a CIMS is softer than the electron impact ionization used in an ACSM and can provide information about the molecular composition of gas-phase species. Ionization by $(H_2O)_{0-2}H_3O^+$ clusters proceeds via either the proton transfer pathway (Eq. 1) or the adduct formation pathway (Eq. 2).

$$R + (H_2O)_n H_3O^+ \rightarrow RH^+ + (n+1)H_2O \quad (1)$$

$$R + (H_2O)_n H_3O^+ \rightarrow R(H_2O)_m H_3O^+ + (n-m)H_2O \quad (2)$$

The sensitivity of the CIMS (e.g., conversion ion intensity of *RH*+ to mass concentration for *R*) depends on the proton affinity of the analyte *R*, the abundance of the reagent ions (i.e., amount of $(H_2O)_{0-2}H_3O^+$ available, the relative distribution of which varies with sample gas humidity as well), and other instrument factors (e.g.,

reaction time scale between reagent ion and analyte, ion transmission efficiencies, etc.) and requires calibration with authentic standards, which are not commercially available or practically viable for the hundreds and possibly more oxidation products observed. The CIMS does not distinguish between isobaric compounds (i.e., compounds with identical molecular compositions but different structures), which may also differ in sensitivities. Secondary ion chemistry of an analyte by a protonated organic analyte may be possible using Equation 3, further complicating product identification. Nonetheless, the CIMS can be used to monitor the trend in gas-phase molecular composition caused by oxidation chemistry with a time-resolution of 1 second.

$$R_1 + R_2H^+ \rightarrow R_1R_2H^+ \quad (3)$$

CELL EXPOSURES

Two polycarbonate modular cell exposure chambers (MIC-101, Billups-Rothenberg, San Diego, CA) were used to house exposed and control samples. Prior to each exposure, the chambers were conditioned with an ozone flush to reduce contamination by plasticizer residues (which were initially found to be responsible for ozone loss), followed by a clean air flush to displace residual ozone. Probes (HMP60, Vaisala, Helsinki, Finland) were used to monitor the RH and temperature downstream from each module. Each module held two or three 6-well plates, and a mix of 0.08-LPM CO_2 (UHP, Airgas, Radnor, PA) and 1.52-LPM VOC–ozone pollutants was pumped through the module for 1 to 4 hours. In parallel, a mix of 0.08-LPM CO_2 and 1.52-LPM humidified clean air was pumped through the control module. The chambers were housed in a temperature-controlled room at 37°C.

RNA EXTRACTION

Immediately after exposure, each membrane was treated with 1 mL of TRIzol (Invitrogen, Carlsbad, CA) on the apical side and gently mixed to ensure thorough lysis. The whole lysate was collected and frozen until the day of the extraction. TRIzol RNA extraction was conducted following the TRIzol manufacturer's instructions with freshly purged ethanol (200 proof, OmniPur, EMD Millipore), isopropanol (molecular biology grade, IBI Scientific, Dubuque, IA), and nuclease-free water (Ambion, Austin, TX) with ultra-high purity N_2. Briefly, TRIzol aliquots were thawed on ice, and 1 mL of chloroform (high-performance liquid chromatography [HPLC] grade, J.T. Baker, Phillipsburg, NJ) was added to induce phase separation. Soluble RNA in the aqueous phase was precipitated in 0.5 mL of isopropanol overnight at -20°C with glycogen (GlycoBlue, Thermo Scientific, Waltham, MA) as a carrier. Following precipitation, the pellet was washed twice with 1 mL 95% ethanol and then air-dried. The purified RNA was incubated with DNAse I (New England Biolabs, Ipswich, MA) following the manufacturer's protocol. The RNA then was reextracted with 200 µL of 25:24:1 mixture of phenol/chloroform/isoamyl alcohol (Fisher BioReagents, Hampton, NH) followed by a chloroform extraction and an isopropanol precipitation as described earlier.

QUANTIFICATION OF 8-oxoG LEVELS IN TOTAL RNA

We quantified 8-oxoG in total RNA using a DNA/RNA Oxidative Damage ELISA (enzyme-linked immunosorbent assay) kit (Cayman Chemical, Ann Arbor, MI). Then 3 µg and 1.5 µg of total RNA were digested with 0.375 µg of nuclease P1 from Penicillium citrinum (Sigma-Aldrich) in 20 mM sodium acetate buffer pH 5.2 containing 50 mM sodium chloride and 0.1 mM zinc chloride in a 105-µL reaction volume. After incubation at 37°C for 2 hours, one unit of calf intestinal phosphatase (New England Biolabs) and 5X alkaline phosphatase buffer (500 mM Tris acetate, 220 mM sodium chloride, and 50 mM magnesium chloride, pH 7.9) were added to a final reaction volume of 150 µL. The ELISA was conducted at two dilutions (1 µg and 0.5 µg of total RNA) with three technical replicates. The levels of free 8-oxoG in RNA were corrected using a factor of 0.38 as suggested in the manufacturer's protocol. Buffers were prepared fresh on the day of the assay using N_2-purged nuclease-free water.

8-oxoG IMMUNOPRECIPITATION AND RNA SEQUENCING

Immunoprecipitation of 8-oxoG–containing RNA was performed in three biological replicates for each condition. After DNase I treatment of RNA, ribosomal RNA (rRNA) was depleted using a Ribo-Zero Gold rRNA Removal kit (Illumina, San Diego, CA) as described by the manufacturer. Depletion of rRNA was validated using an Agilent 2100 Bioanalyzer (Agilent, Santa Clara, CA), and all samples had an RNA integrity number (RIN) higher than 7. All buffers were prepared fresh from concentrated stocks on the day of pulldown experiments. RNA was incubated with 12.5 µg of monoclonal antibody that detects the most common oxidized guanine species (i.e., 8-hydroguanine and its favored tautomeric form 8-oxoG) (Schurch et al. 2016) (0.5 mg/mL, Clone 2E2, Trevigen, Gaithersburg, MD) in IP buffer (10 mM Tris pH 7.4, 150 mM NaCl, 0.1% IGEPAL, and 200 units/mL of SUPERase•In RNase inhibitor) (Invitrogen) in a 1-mL reaction volume for 2 hours on a rotator at 4°C. SureBeads Protein A magnetic beads

(Biorad, Hercules, CA) were then washed according to the manufacturer's recommendation and blocked in IP buffer supplemented with 0.5 mg/mL bovine serum albumin for 2 hours at room temperature. After washing the beads twice in IP buffer, they were resuspended in IP buffer, mixed with the RNA-antibody reaction and incubated for 2 hours on a rotator at 4°C. Next, the beads were washed thrice in IP buffer before performing two competitive elutions with free 8-hydroxy-2′-deoxyguanosine nucleosides (8-OH-dG) (Cayman Chemical), which is a tautomeric form of 8-oxoG deoxyribonucleotides. Each elution was conducted by incubating the beads with 108 μg of 8-OH-dG in IP buffer for 1 hour on a rotator at 4°C. The elution volume was then cleaned using the RNA Clean and Concentrator-5 kit (Zymo Research, Irvine, CA).

Input RNA and immunoprecipitated 8-oxoG–containing RNA libraries were prepared using the NEBNext Small RNA Library Prep kit (New England Biolabs) by the Genomic Sequencing and Analysis Facility at the University of Texas at Austin. Sequencing was performed on an Illumina HiSeq 4000 with a read depth of 16 million reads for pulldowns and 32 million reads for input RNA samples.

ENRICHMENT ANALYSIS

Enrichment analysis of the differentially upregulated, downregulated, and oxidized transcript lists was performed using the Enrichr web tool (Chen et al. 2013; Kuleshov et al. 2016). We generated the lists for enrichment by filtering the transcripts with adjusted P value < 0.05 and fold change > 2 (for upregulated genes) and < 0.5 (for downregulated genes). The list of oxidized genes was obtained for enriched genes (positive fold change) and with an adjusted P value < 0.05. The top 10 pathway enrichment was generated by combining the resulting enriched terms from the Kyoto Encyclopedia of Genes and Genomes (KEGG), WikiPathways, and Panther databases and ranking them by the Enrichr's combined score. Similarly, the top 10 gene ontology (GO) terms resulted from the combination and ranking of all the cellular component, molecular function, and biological process terms.

CONFOCAL MICROSCOPY

Prior to treatment of the cells, membranes were removed from the plastic insert by making an incision around the edge of the membrane. Each membrane was then placed onto a microscope slide mounted in a Petri dish with cells facing upward. Cells were fixed in 1 mL of 3.7% formaldehyde solution in phosphate buffer solution pH 7.4 (PBS, Thermo Fisher Scientific, Waltham, MA) for 15 minutes at 37°C. After fixation, the formaldehyde solution was discarded, and the membrane was washed three times with 1 mL of phosphate buffer solution (PBS) prewarmed to 37°C. Then 1 mL of 0.1% Triton-X-100 (Sigma-Aldrich) in PBS was placed onto the membrane for 4 minutes and washed with 1 mL PBS three times. The membrane was then pre-incubated with 1 mL of 1% bovine serum albumin in PBS for 20 minutes, prior to adding the phallotoxin staining solution. To stain F-actin in the cells, 10 μL of Alexa Fluor 594 Phalloidin solution (Thermo Fisher Scientific) was diluted into 400 μL of PBS with 1% bovine serum albumin solution. The staining solution was placed on the membrane for 20 minutes at room temperature and protected from light to prevent photobleaching. The fluorescent medium was aspirated and washed three times with PBS. Once each membrane was stained, a drop of ProLong Gold Antifade Mountant with DAPI dye (Thermo Fisher Scientific) was placed onto the membrane. A coverslip was positioned on top of the membrane, and then the edges of each coverslip were sealed with clear nail polish and left to dry. Specimens were stored in the dark at 4°C until the day of analysis. Confocal microscopy for analysis was performed using a confocal laser scanning microscope (LSM 710, Carl Zeiss, Jena, Germany). Five or more images were acquired at random locations and captured using Zen Pro software (Carl Zeiss) with a 63× oil objective and filters for the DAPI and Alexa Fluor 594 dyes.

LDH ANALYSIS

Colorimetric Assay

Immediately after exposure, the basolateral medium from each well was collected and frozen at –80°C until the day of analysis. Cellular membrane damage was measured by detection of lactate dehydrogenase (LDH) in the cellular medium using a colorimetric assay (LDH Cytotoxicity Detection Kit, Takara Bio, Mountain View, CA). Absorbance of the assay was measured at 491 nm for 30 minutes at 25°C using a Cytation 3 plate reader (Biotek, Winooski, VT).

Quantitative Label-Free Detection

The 30 μL of basolateral cellular medium collected shortly after three independent VOC–ozone mixture exposures was dissolved in 5% 2-mercaptoethanol sample buffer (3× buffer: 0.5M Tris-HCl pH 6.8, 10% [w/v] sodium dodecyl sulfate [SDS], 25% glycerol, and 0.5% [w/v] bromophenol blue) followed by electrophoresis in 10% polyacrylamide gels at 90V for 15 minutes. After electrophoresis, each band was cut from the gel and chopped into 1- to 2-mm cubes. The gel pieces were incubated for 30 minutes in de-staining solution (50% methanol, 5% acetic acid), washed with deionized water, and de-stained

overnight. Following de-staining, the gel pieces were dehydrated with 100% acetonitrile for 10 minutes and then air-dried in a vacuum centrifuge (Vacufuge Concentrator, Eppendorf, Hamburg, Germany). The gel pieces were then incubated for 45 minutes in 10 mM dithiothreitol at 55°C. The supernatant was discarded, and 55 mM of iodoacetamide was added and incubated for 30 minutes at room temperature in the dark. The gel pieces were washed with 50% acetonitrile and 25 mM ammonium bicarbonate for 15 minutes with constant shaking; this procedure was done twice. To dehydrate the gel, 100% acetonitrile was added for 10 minutes, and then the gel pieces were air-dried for 15 minutes.

Proteins were digested in-gel with Pierce Trypsin Protease, MS grade (Thermo Fisher Scientific), in a final concentration of 10-µg/mL trypsin for 1 hour. The gel pieces were then incubated in 25 mM of ammonium bicarbonate overnight. The supernatant-containing peptides were transferred to a clean tube. To maximize peptide recovery, we incubated the gel pieces with 5% formic acid for 15 minutes, followed by 100% acetonitrile for an additional 15 minutes. Supernatants were combined and submitted to the Center for Biomedical Research Support's Proteomics Facility at the University of Texas at Austin for protein identification by liquid chromatography tandem mass spectrometry (LC-MS/MS), using a Dionex UltiMate 3000 RSLCnano liquid chromatography system (Thermo Fisher Scientific) coupled to an Orbitrap Fusion mass spectrometer (Thermo Fisher Scientific). Prior to HPLC separation, the peptides were desalted using pipette tips (U-C18 ZipTip Pipette Tips, EMD Millipore) following the manufacturer's protocol. A 2-cm-long × 75-µm-internal-diameter C18 trap column was followed by a 25-cm-long × 75-µm-internal-diameter analytical column packed with C18 3-µm material (Thermo Acclaim PepMap 100, Thermo Fisher Scientific). The Fourier transform mass spectrometer resolution was set to 120,000, and 3-second-cycle-time tandem mass spectrometry was acquired in the ion trap mode. Raw data were processed using SEQUEST HT software embedded in Proteome Discoverer software (Thermo Fisher Scientific). Scaffold software (Proteome Software, Portland, OR) was used for validation of peptide and protein identifications with filtering to achieve 99% protein confidence (i.e., a 1% false discovery rate). Statistical significance and fold change were established in Scaffold with a Fisher's exact test using weighted spectra.

WESTERN BLOTTING AND CHOLESTEROL ANALYSIS

Cells attached to the cell culture inserts were lysed by adding 200 µL of M-PER mammalian protein lysis buffer (Thermo Scientific) supplemented with Halt protease inhibitor cocktail (Thermo Scientific) with vigorous mixing by pipetting. The lysate was stored at –80°C until the day of analysis, and protein concentrations were analyzed using the Coomassie (Bradford) protein assay kit (Thermo Scientific). The whole protein lysate was dissolved in 5% 2-mercaptoethanol sample buffer (3× buffer: 0.5M Tris-HCl pH 6.8, 10% [w/v] SDS, 25% glycerol, and 0.5% [w/v] bromophenol blue). Electrophoresis of 0.5–5 µg of protein loaded per lane was conducted in 10% polyacrylamide gels at 90V for 2.5 hours. Protein bands in the gel were transferred to 0.2-µm nitrocellulose membranes (Biorad) using a Trans-Blot SD Semi-Dry Transfer Cell (Biorad). The membranes were then blocked overnight in 5% skimmed milk in Tris-buffered saline containing 0.05% Tween 20. FDFT1 was detected with rabbit monoclonal anti-FDFT1 IgG [EPR16481] (ab195046, Abcam, UK) used at 1:5,000 dilution. Goat anti-rabbit IgG H&L HRP conjugate (ab6721, Abcam) was used as secondary antibody at 1:10,000 dilution. Immunodetection was performed with the Clarity Western enhanced-chemiluminescence substrate (Biorad). Prior to detection of glyceraldehyde 3-phosphate dehydrogenase (GAPDH) as the loading control, the membrane was stripped with mild stripping buffer (200 mM glycine, 0.1% [w/v] sodium dodecyl sulfate (SDS), and 1% Tween 20) and then blocked and reblotted using mouse monoclonal GAPDH Antibody [6C5] (Santa Cruz Biotechnology, Dallas, TX). Polyclonal anti-mouse IgG H&L HRP conjugate (Promega, Madison, WI) was used as secondary antibody. Chemiluminescent detection was conducted on a ChemiDoc XRS+ imaging system (Biorad) and quantification of the band's intensity with CLIQS software (TotalLab, UK).

Intracellular cholesterol was quantified in whole cellular lysates using the Amplex Red Cholesterol Assay kit (Thermo Scientific) according to the manufacturer's instructions. Cholesterol was measured in two biological replicates, and each sample was quantified in triplicate.

IMAGE ANALYSIS

The extent of F-actin area was quantified in Fiji/ImageJ software by drawing the outline of the cell with the freehand pencil tool in at least five cells in three confocal images (63× magnification) selected for each biological replicate and condition. The F-actin organization around the nucleus and plasma membrane was quantified using the Fibriltool plugin in Fiji according to the described protocol (Boudaoud et al. 2014). This analysis was conducted in three confocal images (63× magnification) selected for each biological replicate and condition. The anisotropic score was computed on five or more cells per image by drawing an area of interest of approximately 5 µm by 10 µm.

The fraction of cells adhered was estimated by computing the area of F-actin for the channel stained with phalloidin. Each image was processed by the color threshold feature in Fiji, and the area of actin coverage was quantified using the particle analyzer tool. To compute the fraction, the resulting cell area was divided by the total area of the image (18,204 μm^2). Three images were selected per condition.

STUDY DESIGN

Experimental Protocol 1

Our initial experiments focused on identifying the duration of the exposure that generated cellular responses similar to the ones described in our previous work with A549 epithelial lung cells (Baldridge et al. 2015). We thus conducted exposures of BEAS-2B cells to the VOC–ozone mixtures with 790 ppb ACR, 670 ppb MACR, and 4 ppm ozone as precursors. Clean air controls were run alongside the VOC–ozone mixtures and an incubator control. Three 6-well plates containing cell culture inserts were placed in two exposure modules, and one module was injected with the VOC–ozone mixtures and the other with clean air for 4 hours. The plates were arranged in the same orientation (with respect to the inlet and outlet ports) for both the module and the control sets. After 1, 2, and 4 hours of exposure, a plate was removed from each module to collect the basolateral medium and to lyse cells with TRIzol. These samples were frozen on dry ice and then transferred to a −80°C freezer for sample analysis the following day. To determine the cytotoxic effect of the exposure duration, we analyzed LDH levels in the basolateral medium. Furthermore, we characterized the incidence of RNA oxidation in RNA extracted from the TRIzol samples. These results are summarized in Additional Materials 1: Appendix A, Figure A.1, on the HEI website at *www.healtheffects.org/publications*.

Experimental Protocol 2

To generate RNA samples for RNA sequencing, we set the duration of the exposure to 1.5 hours based on the results from experimental protocol 1. We conducted three independent VOC–ozone exposures on different days alongside clean air controls. Before preparing samples for 8-oxoG immunoprecipitation, we confirmed expected trends in the levels of LDH and 8-oxoG. RNA extractions from independent cell culture inserts were treated with DNase and then depleted of rRNA. Analysis of RNA integrity was assessed by bioanalyzer before conducting 8-oxoG immunoprecipitation. Each rRNA-depleted sample consisting of a total volume of 2 μL was split into 1 μL for 8-oxoG pulldown and 1 μL for the nonenriched library sample preparation. The nonenriched library sample is the pool of RNAs before 8-oxoG immunocapture and represents the endogenous density of transcripts on each condition. Both RNA pools (8-oxoG enriched and nonenriched) from three independent exposures and clean air controls were submitted for RNA sequencing.

Experimental Protocol 3

We conducted two additional biological replicates of the VOC–ozone exposures alongside clean air controls to characterize expression levels of proteins encoded by specific mRNAs prone to oxidation in BEAS-2B cells. Exposures were conducted for 1.5 hours, and cells were immediately lysed with a buffer formulated for extraction of mammalian proteins (M-PER, Fisher Scientific). Whole lysates were frozen in dry ice and transferred to a –80°C freezer for sample analysis the following day. We analyzed protein levels in the whole lysate from two independent exposures and loaded 0.5 to 5 μg of lysate in a polyacrylamide gel. After gel electrophoresis and protein transfer from the gel to a membrane, the membrane was blotted for detection of the target protein and then stripped and reblotted for detection of the loading control protein. We selected GAPDH as the loading control after confirming similar levels of the GAPDH encoding mRNA and of the GAPDH protein across all exposure conditions (VOC–ozone and clean air) by real-time quantitative polymerase chain reaction and western blot, respectively. In addition to analyzing mRNA and protein levels, we quantified cholesterol levels on the whole cell lysate (containing all the cellular proteins) used for western blotting.

For the microscopy analysis, we conducted two independent time-course exposures with duplicates alongside clean air controls. After cell exposures for 1.5 hours, two membranes for each condition were removed from the plastic insert and treated with 1 mL of 3.7% formaldehyde in Petri dishes. In four additional cell culture inserts for each condition, we exchanged the medium and incubated cells at 37°C and 5% CO_2 for 6 hours and 18.5 hours. At each time point, two membranes per condition were treated with 1 mL of 3.7% formaldehyde, incubated with specific fluorophores (DAPI and Alexa Fluor 594 phalloidin), and sealed with nail polish between a microscope slide and a coverslip. All the membranes were maintained light-protected at 4°C and visualized within 2 weeks after the exposure.

STATISTICAL METHODS AND DATA ANALYSIS

We conducted statistical analysis of differential expression and 8-oxoG enrichment from three biological replicates using the DESeq2 software package (Love et al. 2014) in R version 3.4.0. This package is the leading tool for estimation of variance mean dependence in count data from high-throughput sequencing assays (Schurch et al. 2016). To select transcripts that were differentially expressed after exposure, the nonenriched RNA pools from three biological replicates for each of the unexposed and exposed conditions were compared using the likelihood ratio test based on a negative binomial distribution implemented by DESeq2. Transcripts with an adjusted P value < 0.05 and a fold change > 2 or < 0.5 were selected. We used adjusted P values calculated by DESeq2 to correct for multiple comparison. For 8-oxoG-enrichment analysis, a paired sample design was used to account for variations in the nonenriched samples in identifying transcripts that were specifically oxidized. We defined the 8-oxoG enriched sample as the RNA pool in the presence of an antibody that selectively binds 8-oxoG containing RNAs, and the nonenriched pool of transcripts as the pool in the absence of any 8-oxoG binding antibody. Transcripts enriched in 8-oxoG modifications were chosen for each condition based on an adjusted P value < 0.05 and a fold change > 2. Importantly, we believe that the 8-oxoG immunocapture was unsuccessful in pulling down RNA in one replicate because the 8-oxoG-enrichment sample failed to produce usable sequencing libraries for both exposed and unexposed groups. Therefore, for the identification of 8-oxoG–enriched reads only two biological replicates were analyzed.

We conducted all described measurements as either biological triplicates or duplicates. All data were presented as the mean ± standard deviation. Statistical analysis between groups was determined by Student's t-test in JMP statistical software (SAS, Cary, NC) with a significance of 0.05.

For transcriptomics analysis, we used FastQC software to generate quality-check reports on the raw data, and then read trimming was performed using Trimmomatic 0.36 software, followed by another quality check using FastQC that demonstrated high-quality read data. These preprocessed data were then aligned to the Ensembl comprehensive human genome annotation system (GENCODE 26, GRCh38.p10) using STAR 2.5.3a software, allowing novel splice junctions and using a two-pass mapping approach (transcriptome reference assembly, then realignment to the reference) for comprehensive transcriptome alignment. Alignment was performed using parameters recommended in the STAR manual for ENCODE standards with a resultant mapping rate of >68% for all samples and multimapping rates of 9%–22%. Next, RNA-Seq by Expectation Maximization was used to estimate transcript abundances, and then differential expression and 8-oxoG enrichment analysis were performed using DESeq2 in R version 3.4.0. Transcripts were annotated using the BioMart database system in R. This package and its processor, DESeq, based on a negative binomial distribution, are the leading tools (based on the number of citations) for assessing quantitative differences between experimental conditions in high-throughput sequencing data (Schurch et al. 2016).

RESULTS

AIM 1

Our efforts to discover specific RNA transcripts in BEAS-2B cells that are affected by VOC–ozone mixtures by way of 8-oxoG RNA modifications brought the following results.

Chamber Analysis of Exposure Conditions

We exposed BEAS-2B cells to acute doses of VOC–ozone mixtures generated from the reaction of ACR and MACR with ozone using the ALI system depicted in Figure 1. VOC precursors and ozone were mixed for 10 minutes inside the environmental chamber (kept at 37°C) before starting the cell exposure. The air mixture before injection into the cell exposure module was characterized using a SEMS, ACSM, and high-resolution time-of-flight CIMS. Probes for temperature and RH (maintained higher than 50% during the 1.5-hour exposure) were positioned in the exit stream from each chamber. Two or three 6-well plates were housed in the preconditioned exposure module. A mixture of 1.52 LPM VOC–ozone and 0.08 LPM CO_2 (5% by volume) was pumped through the exposure module for 1.5 hours. In parallel, 1.6 LPM of humidified clean air (5% CO_2 by volume) was pumped through the control. The loss of ozone between the mixing chamber and the exposure module was estimated to be 80%, likely caused by reactions of ozone with the cell culture medium. Ozone loss was calculated by sampling ozone alternately at the inlet and outlet of the exposure chambers (the difference between the inlet and outlet concentrations being the loss). The chambers were conditioned with high ozone concentrations one day before the experiment; thus, we expect that most of the loss is due to the culture, not the chamber itself. The loss of ACR and MACR was less than 20%. Overall, the cells were exposed to unreacted VOCs (ACR and MACR) and ozone as well as VOC–ozone reaction products.

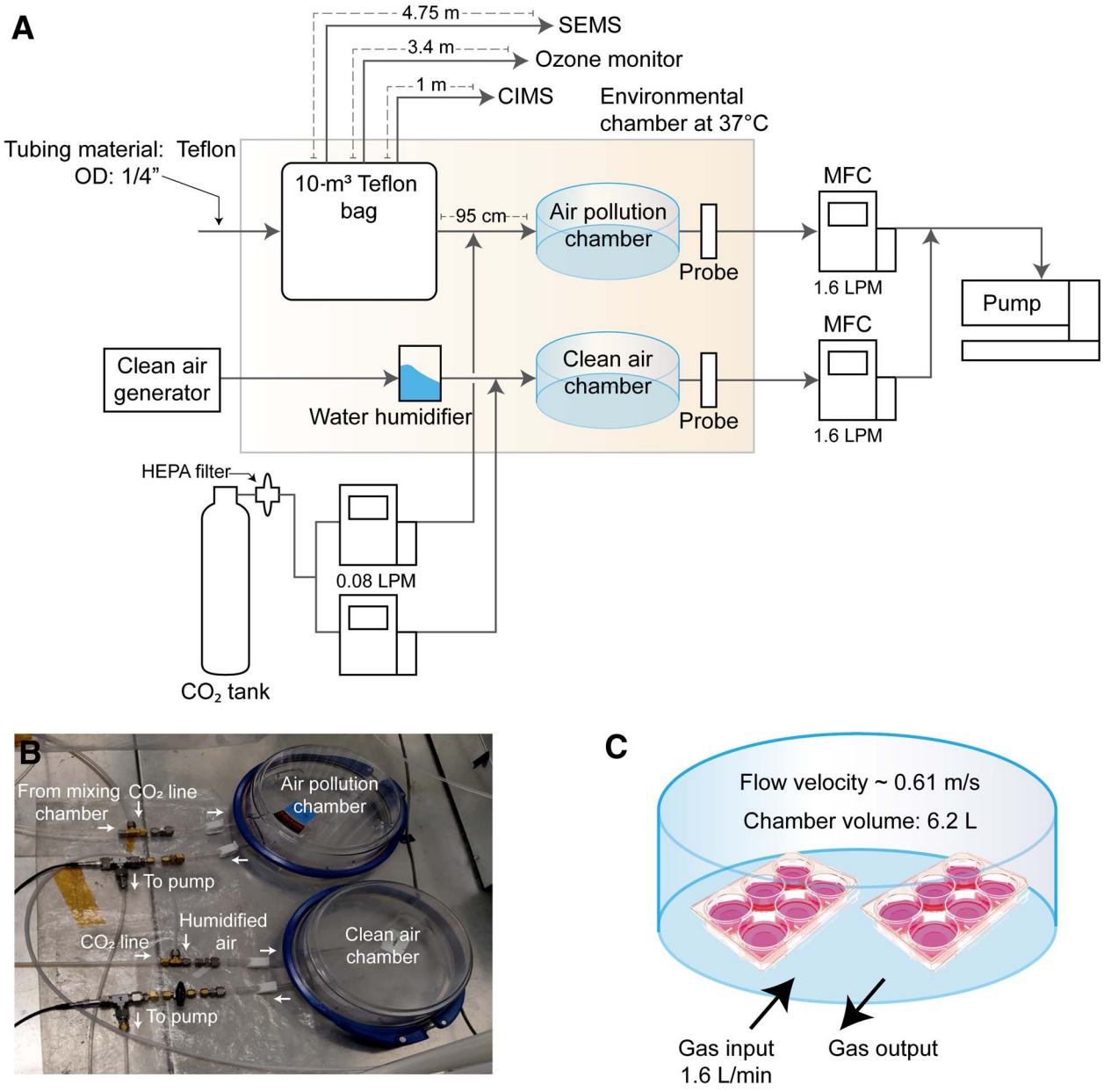

Figure 1. Schematic of the exposure setup: (A) ALI exposure system, consisting of a temperature-controlled environmental chamber containing a 10-m^3 Teflon bag and two cell-exposure modules. Particle filters were placed in-line before CO_2 injection, and probes were used to monitor the temperature and RH inside each module; **(B)** analytical instruments located outside of the chamber; and **(C)** location of the injection and withdrawal ports in the modules.

Typical experimental profiles for real-time levels of gaseous precursors, aerosol concentrations, and reaction-product compositions in the gas and particle phases are shown in Figure 2. We observed the decay of ACR and MACR precursors in the presence of ozone (Figure 2A). Ozone reacts with unsaturated hydrocarbons via the Criegee intermediate reaction mechanism, where ozone adds to and cleaves the olefinic double bond, producing smaller (i.e., compounds with fewer carbon atoms) aldehyde and ketone as well as hydroperoxyl and alkyl peroxyl radicals in the process (Ren et al. 2017). As shown in Figure 2C, we observed oxidation products with more

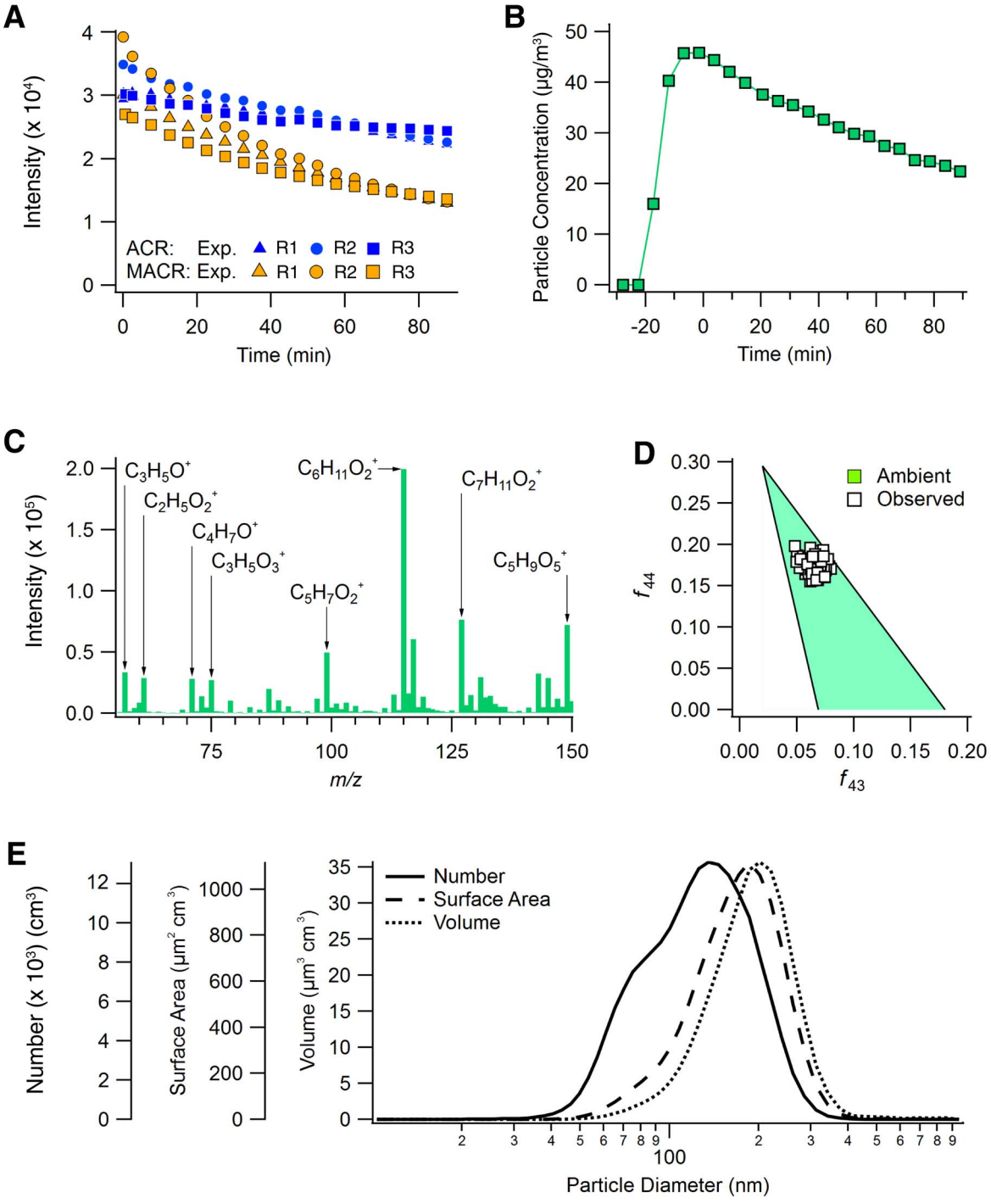

Figure 2. Physicochemical characterization of the VOC–ozone mixture: (A) Decay of ACR and MACR for three independent experiments as observed by high-resolution time-of-flight CIMS. Five-minute averages are shown. **(B)** Typical time-series profile of secondary organic aerosol concentrations as observed by ACSM. Five-minute averages are shown. **(C)** Gas-phase composition observed during the exposure period using CIMS. Average integrated unit-mass ion intensities are shown. Labels indicate selected dominant ions observed at the corresponding *m/z*. Ions ranging from *m/z* 2–56 to 151–400 were monitored but not shown. Precursor VOCs were detected as $C_3H_5O^+$ (ACR, C_3H_4O) and $C_4H_7O^+$ (MACR, C_4H_6O). Because of a lack of authentic standards for oxidation products, the ion intensities shown were not adjusted for sensitivities. **(D)** Typical f_{43} versus f_{44} profile as observed by ACSM. **(E)** Size distribution of secondary organic aerosol as observed by SEMS, averaged over the exposure period. Lognormal distributions are shown. (Panels C, D, and E from Gonzalez-Rivera et al. 2020 Supplementary figures a,b,c [Creative Commons Attribution 4.0 International License].)

carbon numbers (i.e., $C_{>5}$ compounds) than were found in the original VOCs, which suggests that $RO_2 + RO_2$ chemistry (which leads to the formation of carbon–carbon bonds) may be important. In addition, OH radicals produced from the ozone chemistry via HO_2 radical formation can also react with ACR and MACR via either OH addition to the olefinic double bond or hydrogen abstraction. Therefore, OH–ACR and OH–MACR reactions products can also be expected from ozone–ACR and ozone–MACR reactions.

The secondary organic aerosol dose generated in the chamber was estimated to be around 32.3 μg/m^3, based on an ACSM collection efficiency of 0.5 (Figure 2B). The decrease in aerosol concentration was caused by loss of suspended particles and organic vapors to the Teflon environmental chamber wall (Huang et al. 2018; Nah et al. 2017). The f_{43} versus f_{44} profile (a proxy for aerosol oxidation state) in Figure 2D fell within the typical range observed in ambient organic aerosol samples (as represented by the shaded region) (Ng et al. 2011). f_{44} and f_{43} approximate the fractional contribution by CO_2^+ and $C_2H_3O^+$ ions, respectively, to the total organic ions produced from electron impact ionization of organic aerosols. Higher f_{44} values are associated with greater contributions by more oxidized compounds (e.g., doubly oxidized compounds) to the aerosol mass; higher f_{43} values are associated with greater contributions by lightly oxidized compounds (e.g., singly oxidized compounds). Results show that ACR–MACR ozonolysis and/or OH-oxidation products resemble highly processed ambient organic aerosol in terms of aerosol oxidation state. The average size distribution shows that the particle-phase reaction products were dominated by fine (particle diameter < 2.5 μm) and ultrafine (particle diameter < 0.1 μm) organic aerosol (Figure 2E)

Cytotoxicity and Total RNA Oxidation Measurements

Our first goal was to evaluate whether the exposure conditions for our VOC–ozone mixtures could generate levels of cellular damage and oxidative stress markers that were distinguishable from those of clean air exposures. Based on our previous studies, we expected these exposure levels to overwhelm cellular defenses and to elicit specific oxidative stress responses (Baldridge et al. 2015). We determined the release of LDH in the BEGM medium on exposure to the VOC–ozone mixtures by a colorimetric assay based on a two-step enzymatic reaction. LDH levels were used as a reporter of membrane integrity, which can be interpreted as a measure of cell death or cellular stress. We observed that LDH levels increased sevenfold (with a significance of P value < 0.05) after exposure of BEAS-2B cells to VOC–ozone mixtures compared with control exposures (Figure 3A), an increment typically associated with minimal cell death in air pollution exposures (Rager et al. 2011). This result is consistent with reported observations in A549 cells treated with similar doses of VOC–ozone mixtures (Baldridge et al. 2015).

These levels were further contrasted with LDH identification by LC-MS/MS to assess whether potential inactivation of the enzyme led to underestimation of the extent of cell death by the biochemical assay. Figure 3B shows the total spectrum counts, accepted as a quantitative measurement of protein abundance in proteomic studies, for the two main subunits of LDH (LDH-A and LDH-B) (Liang et al. 2016) in the samples exposed to VOC–ozone and clean air control using LC-MS/MS. The LDH counts increased approximately eight units in the exposed cells as compared to the clean air control cells, in which the LDH subunits were not detected. Furthermore, these results suggest that comparable levels of LDH release were detected by both LC-MS/MS and the biochemical methods (Uhlen et al. 2017).

In addition to measuring cellular damage, we conducted an analysis of the accumulation of 8-oxoG in total RNA. As a marker of oxidative stress, 8-oxoG has been widely quantified in vivo and in vitro for evaluation of the genotoxic effect of atmospheric agents (Andreoli et al. 2015; Baldridge et al. 2015; Nehls et al. 1997). We extracted RNA and quantified the concentration of free 8-oxoG ribonucleotides in nuclease-treated total RNA by ELISA. We observed that free 8-oxoG levels increased in total RNA by 1.7-fold on exposure compared with the control. Similar trends have been detected in VOC–ozone exposures in A549 cells (Baldridge et al. 2015).

Transcriptomics Analysis in BEAS-2B Cells after Exposure to VOC–Ozone Mixtures

We conducted differential expression analysis of BEAS-2B cells exposed to VOC–ozone mixtures for 1.5 hours in an ALI system. Cells exposed to the VOC–ozone mixtures showed differential expression of 266 transcripts (adjusted P value < 0.05), 153 with increased expression (fold change >2) and 113 with decreased expression levels (fold change ≤ -2) (Figure 4A and Tables B.1 and B.2 in Additional Materials 2: Appendix B, on the HEI website at *www.healtheffects.org/publications*). To identify potential biological pathways affected by air pollution exposure, we performed pathway enrichment analysis using Enrichr for the upregulated and downregulated gene sets (Figures 5 and 6). For the upregulated genes, we observed enrichment of interesting

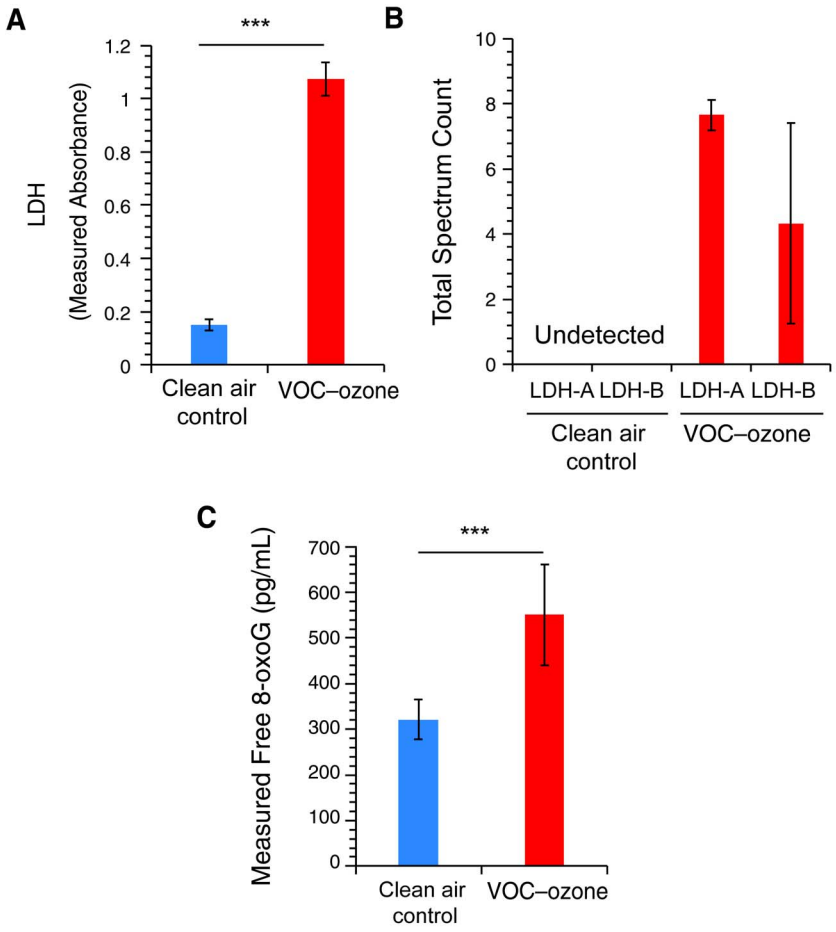

Figure 3. Levels of biomarkers shortly after exposure to the VOC–O_3 mixture, showing increases in LDH and 8-oxoG levels in total RNA: **(A)** LDH levels in the basolateral media detected by a colorimetric assay based on enzymatic activity. **(B)** LDH levels in the basolateral media as detected by LC-MS/MS. **(C)** Free 8-oxoG ribonucleotide levels as detected by ELISA from total RNA. Statistical differences were computed using *t*-test analysis. Significance is denoted as *** for P values < 0.0005.

pathways, such as several cellular signaling pathways, bacterial invasion, cell-to-cell and extracellular matrix adhesion, and Alzheimer's disease. For the downregulated genes, we observed apoptosis, longevity regulation, oxidative stress, and several pathways related to diseases. We also analyzed GO terms using Enrichr to identify biological processes, cellular components, and molecular functions associated with the upregulated and downregulated genes. We found that upregulated genes were associated with binding to transmembrane protein, cell adhesion, and the lumen of the endoplasmic reticulum. The downregulated genes represented terms linked to regulation of proliferation in various tissues, regulation of transcription, and protein ubiquitination.

Transcriptomics Analysis of RNA Oxidation in BEAS-2B Cells after Exposure to VOC–Ozone Mixtures

Given that RNA oxidations have been hypothesized as early events in the time course of cellular damage and are potentially more sensitive to environmental stress

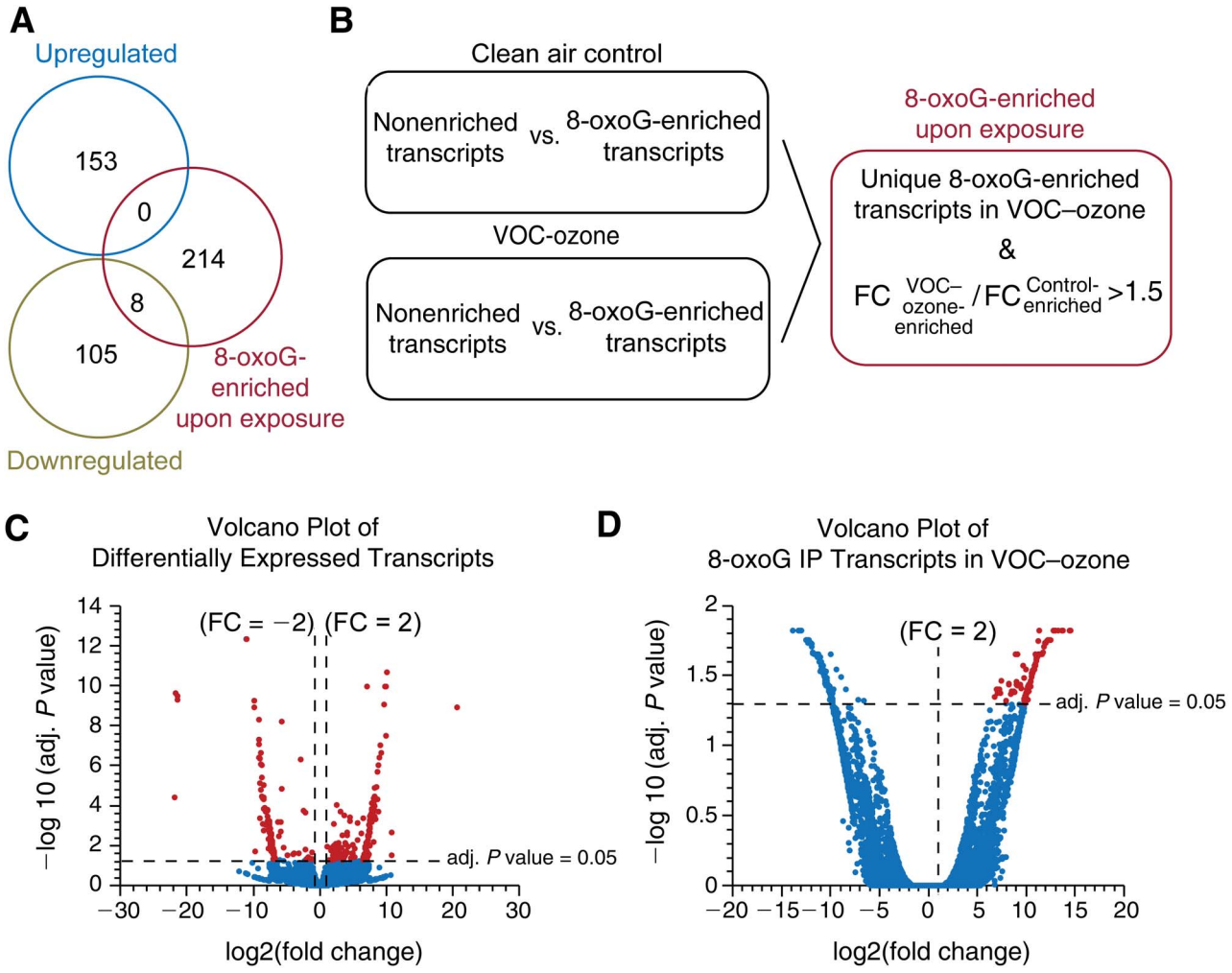

Figure 4. Transcript expression profiling showing that certain RNAs are more prone to oxidation: (A) Venn diagram showing the number of transcripts upregulated and downregulated on exposure of BEAS-2B cells to VOC–O_3 mixtures, and the overlap with the eight transcripts identified as being significantly sensitive to oxidation upon exposure. **(B)** Significantly oxidized transcripts after exposure to VOCs–O_3, identified by comparing the enrichment of 8-oxoG by immunoprecipitation with the nonenriched pool of transcripts. **(C)** Volcano plot showing differentially expressed transcripts after exposure to the VOC–O_3 mixture (shown in red). **(D)** Volcano plot showing transcripts enriched in RNA oxidation (shown in red) induced by the VOC–O_3 mixture. FC indicates fold change.

(Nunomura et al. 2001, 2006) than other macromolecules (i.e. DNA or proteins), oxidation-prone transcripts can serve as consistent markers of exposure. Furthermore, oxidation-prone transcripts have the potential to reveal affected pathways and cellular mechanisms not detected by gene expression profiling. As such, we integrated immunoprecipitation of 8-oxoG–containing RNAs with transcriptomics to identify specific transcripts susceptible to 8-oxoG modifications after air pollution exposures. This approach has been used successfully for identification and localization of methylated mRNA, such as N^6-methyladenosine and 1-methylguanosine, under various physiological conditions (Li et al. 2016). We identified significantly oxidized transcripts after exposure to the VOC–ozone mixtures by analyzing the relative transcript abundance of 8-oxoG and the relative abundance of basal 8-oxoG–containing transcripts in the control samples (because a basal level of cellular oxidation is present in cells even in the absence of any oxidative environmental stressor) (see Additional Materials 1: Appendix A, Figure A.2). Hence, we selected

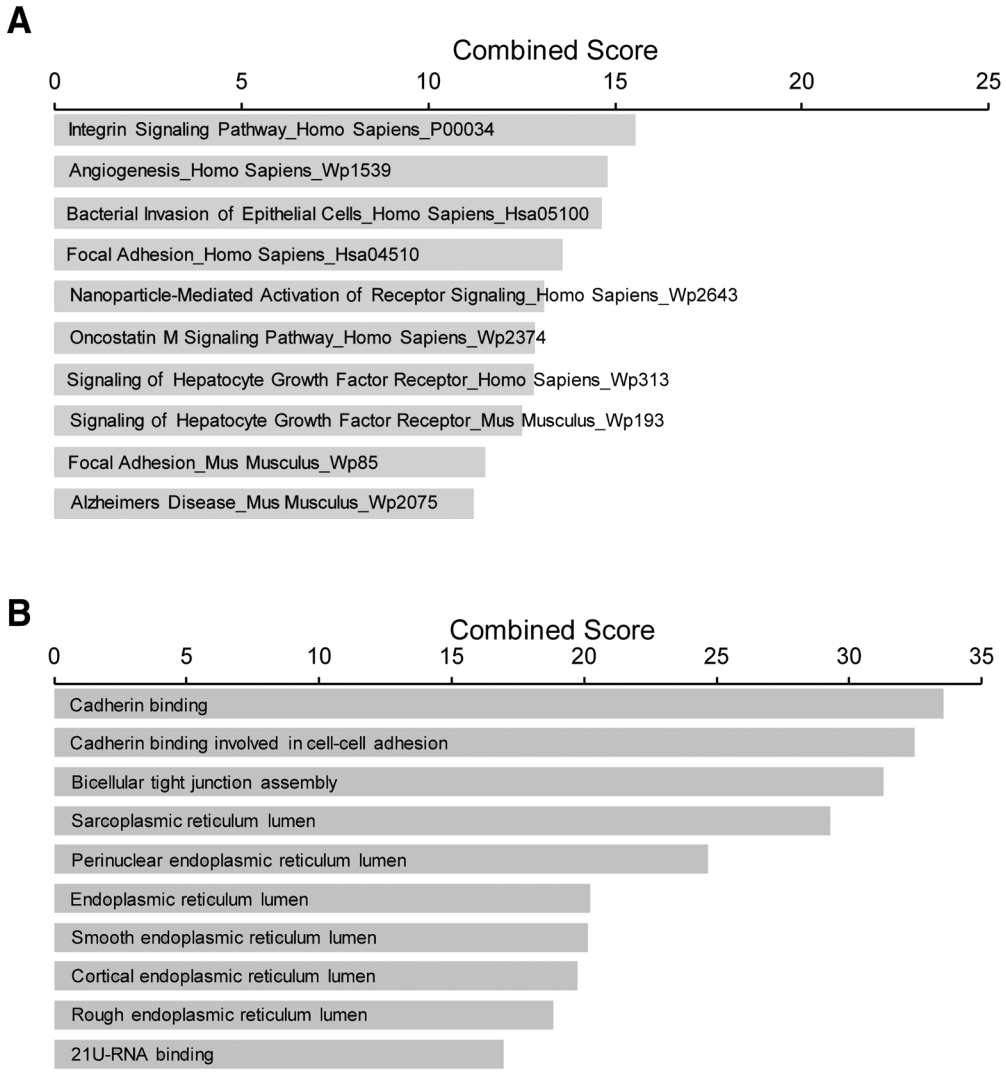

Figure 5. Top 10 pathways (A) and GO terms (B) enriched from the differentially upregulated transcripts. Terms were ranked by the combined score in Enrichr. Genes associated with each pathway and GO term are presented in Appendix B, Tables B.4 and B.5, respectively.

unique 8-oxoG transcripts in the exposed samples as well as transcripts that were present in both the VOC–ozone-exposed and clean air control pools with an exposed-to-control fold-change ratio higher than 1.5 (Figure 4B). We identified 222 transcripts significantly enriched in 8-oxoG on exposure (Table B.3 in Additional Materials 2: Appendix B); this was interpreted as transcripts that were highly susceptible to RNA oxidation via the oxidative environment generated by the pro-oxidant VOC–ozone mixtures in the BEAS-2B cells (Figure 4D). As seen in Figure 4A, only eight significantly oxidized transcripts were identified as downregulated transcripts, and no oxidized transcripts were upregulated (Table). Interestingly, we found genes associated with nuclear matrix support (nesprin-2 and prelamin-A/C) and transcription regulation (ATP-dependent RNA helicase DDX3X) with more than one of these three transcript isoforms highly prone to oxidation.

To characterize the biological relevance of the specific mRNA oxidation observed, we performed enrichment pathway analysis in the oxidized transcript set to identify

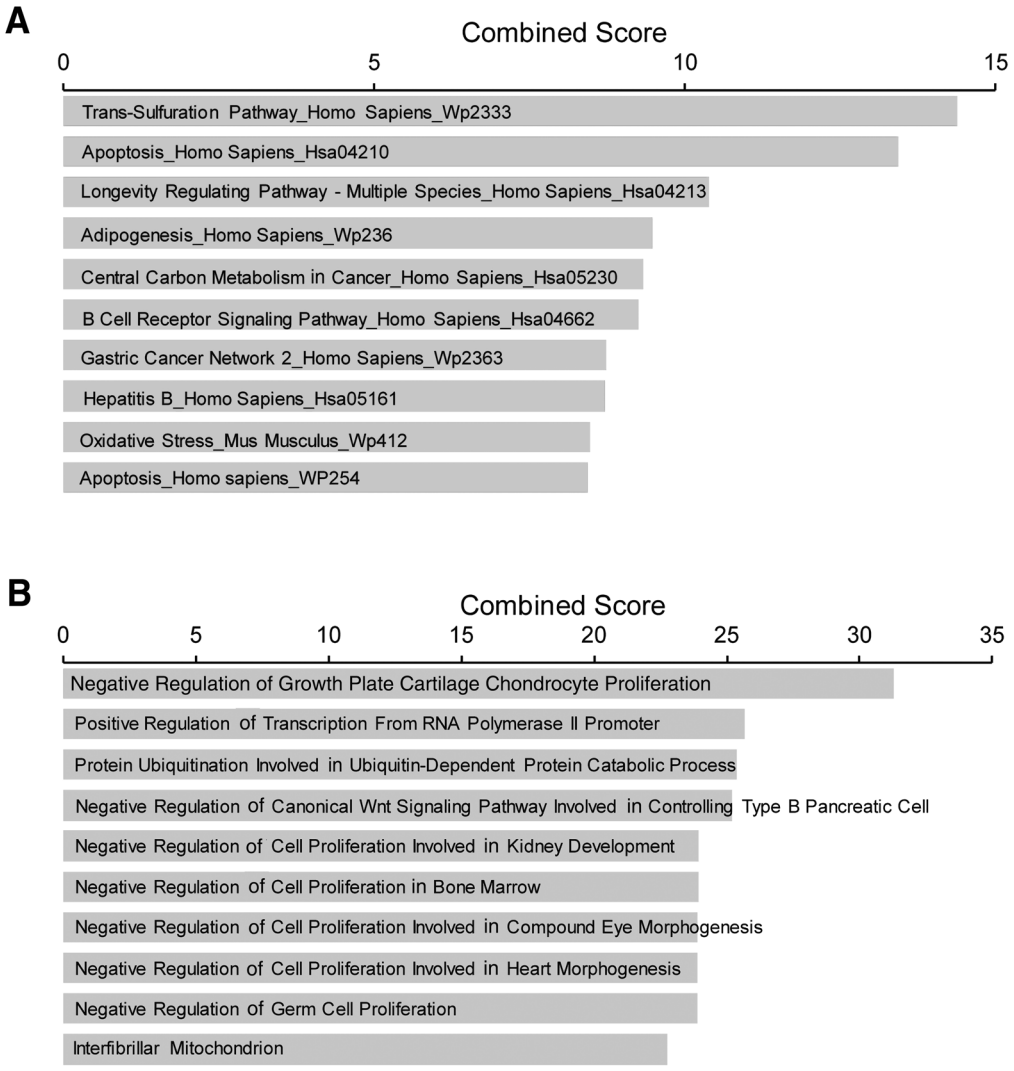

Figure 6. Top 10 pathways (A) and GO terms (B) enriched from the differentially downregulated transcripts. Terms were ranked by the combined score in Enrichr. Genes associated with each pathway and GO term are presented in Appendix B, Tables B.6 and B.7, respectively.

specific molecular functions that were affected (Figure 7). We observed some overlapping between the mRNAs enriched in the set of differentially expressed transcripts (between VOC–ozone and clean air conditions) and the mRNAs enriched in 8-oxoG upon exposure; these included mRNAs in the bacterial invasion and focal adhesion pathways. Among the functions exclusively affected by RNA oxidation, we found signaling networks such as the EGFR signaling pathway as well as translational regulation and cytoskeleton elements and regulators. As a note, mRNAs enriched in 8-oxoG refer to the mRNA pool in the presence of an antibody that selectively binds 8-oxoG–containing RNAs; we can therefore interpret these as transcripts that are highly susceptible to oxidation on exposure.

AIM 2

Our efforts to mechanistically characterize the adverse effects of pro-oxidant air from VOC–ozone mixtures on membrane and cytoskeleton integrity of lung cells via 8-oxoG RNA modifications brought the following results.

Table. Eight Significantly Oxidized and Downregulated Transcripts

Gene	Transcript Biotype	Gene Description	UniProt Function
DGLUCY	Protein coding	D-glutamate cyclase, mitochondrial	Converts D-glutamate to 5-oxo-D-proline.
DNMT1	Protein coding	DNA methyltransferase 1	Methylates CpG residues. Preferentially methylates hemimethylated DNA. Associates with DNA replication sites in S phase maintaining the methylation pattern in the newly synthesized strand, which is essential for epigenetic inheritance. Associates with chromatin during G2 and M phases to maintain DNA methylation independently of replication.
FDFT1	Nonsense-mediated decay (NMD)	Farnesyl-diphosphate farnesyltransferase 1	Encodes a membrane-associated enzyme located at a branch point in the mevalonate pathway. The encoded protein is the first specific enzyme in cholesterol biosynthesis, catalyzing the dimerization of two molecules of farnesyl diphosphate in a two-step reaction to form squalene.
LMNA	Protein coding	Prelamin-A/C	Lamins are components of the nuclear lamina, a fibrous layer on the nucleoplasmic side of the inner nuclear membrane, which is thought to provide a framework for the nuclear envelope and may also interact with chromatin. Plays an important role in nuclear assembly, chromatin organization, nuclear membrane, and telomere dynamics.
PTPRK	Protein coding	Receptor-type tyrosine-protein phosphatase kappa	Regulation of processes involving cell contact and adhesion such as growth control, tumor invasion, and metastasis. Negative regulator of EGFR signaling pathway.
TEDC2	Protein coding	Tubulin epsilon and delta complex 2	Uncharacterized protein.
TRIM39	Protein coding	E3 ubiquitin-protein ligase TRIM39	May facilitate apoptosis by inhibiting APC/C-Cdh1-mediated poly-ubiquitination and subsequent proteasome-mediated degradation of the pro-apoptotic protein MOAP1.
USP40	Protein coding	Ubiquitin carboxyl-terminal hydrolase 40	May be catalytically inactive.

To elucidate the adverse effects of VOC–ozone that can help explain a fundamental mechanistic basis of diseases, we analyzed phenotypes from the pathways affected by exposure of BEAS-2B cells to VOC–ozone mixtures. Given that the functional analysis of oxidized transcripts revealed multiple pathways, many related to the integrity and dynamics of the cytoskeleton, we acquired confocal microscopy images of the cytoskeletal actin fibers to elucidate the response of cytoskeleton activity under stress. We exposed BEAS-2B cells for 1.5 hours to VOC–ozone mixtures and analyzed the dynamic organization of F-actin immediately before (t = 0) and after (t = 1.5 h) exposure, in addition to 7.5 hours and 20 hours of cell recovery after exposure (Figure 8A). We stained F-actin with phalloidin Alexa 594 and the nuclei with DAPI and observed that the structure, orientation, and density of the actin filaments were consistent in the clean air control at all time points in the experiment. The actin filaments, for example, looked linear and well organized in parallel arrays. As expected, we saw accumulation of F-actin near the cell periphery, and the cells maintained typical BEAS-2B

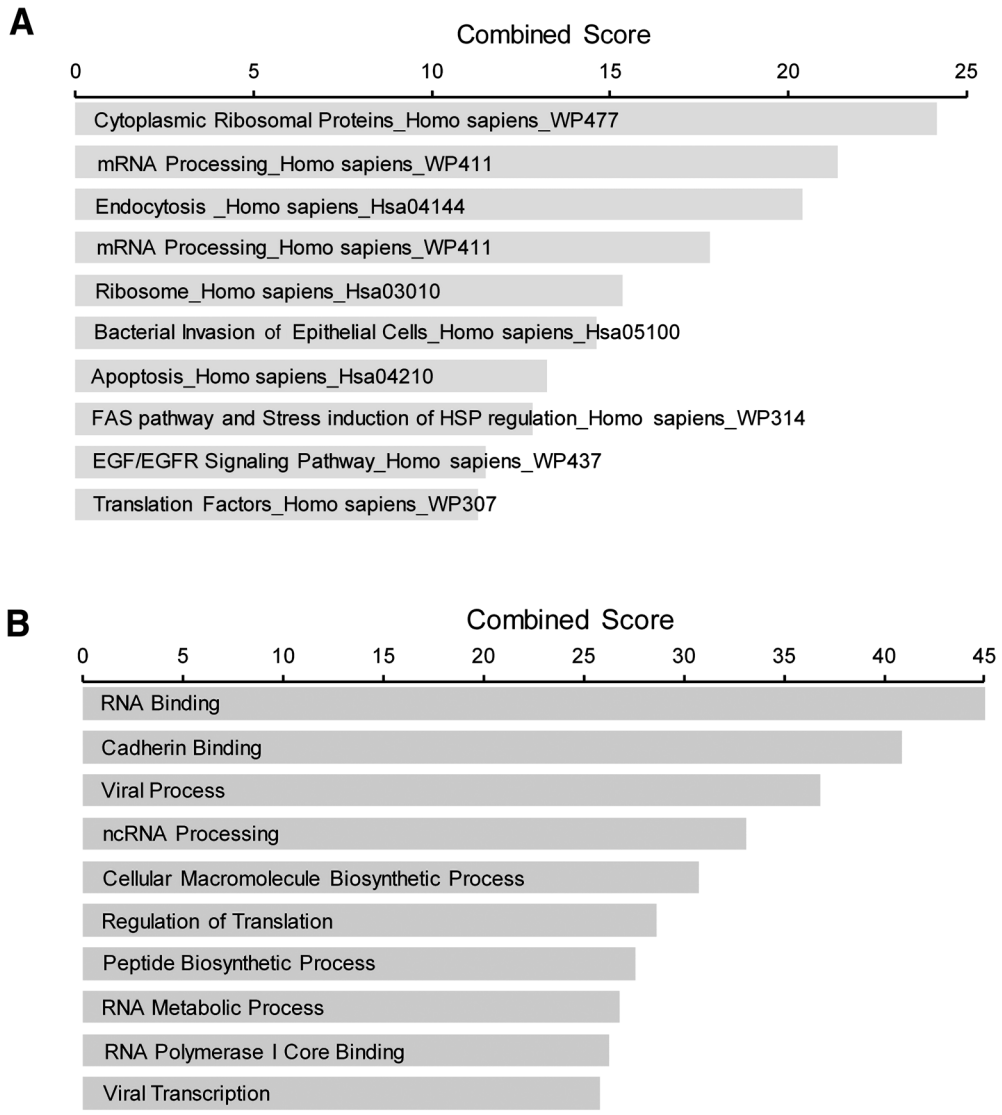

Figure 7. Top 10 pathways (A) and GO terms (B) enriched from the oxidized transcripts upon exposure. Terms were ranked by the combined score in Enrichr. Genes associated with each pathway and GO term are presented in Appendix B, Tables B.8 and B.9, respectively.

morphology when cultured below confluency. These observations provided a baseline for recognizing the structure and organization of F-actin under healthy physiological conditions. Further, we confirmed cell viability by inspecting cells using a widefield fluorescent microscope with a magnification of 10×; the images showed an increase in clean air control cell density over time, and cells reached confluence at $t = 20$ hours in the clean air control cells (Additional Materials 1: Appendix A, Figure A.4, on the HEI website at *www.healtheffects.org/publications*).

When we exposed the BEAS-2B cells to the VOC–ozone mixtures, the cells presented irregular shapes, fibers became twisted, and bright globules of phalloidin formed, suggesting fiber disintegration and aggregation as early as 1.5 hours (Figure 8A).

We then quantified the extent of F-actin using Fiji/ImageJ on the confocal fluorescent microscopy images. The area covered by actin filaments can be used as a measured of cytoskeleton rearrangements and integrity (Figure 8B). We observed that the extent of F-actin remained

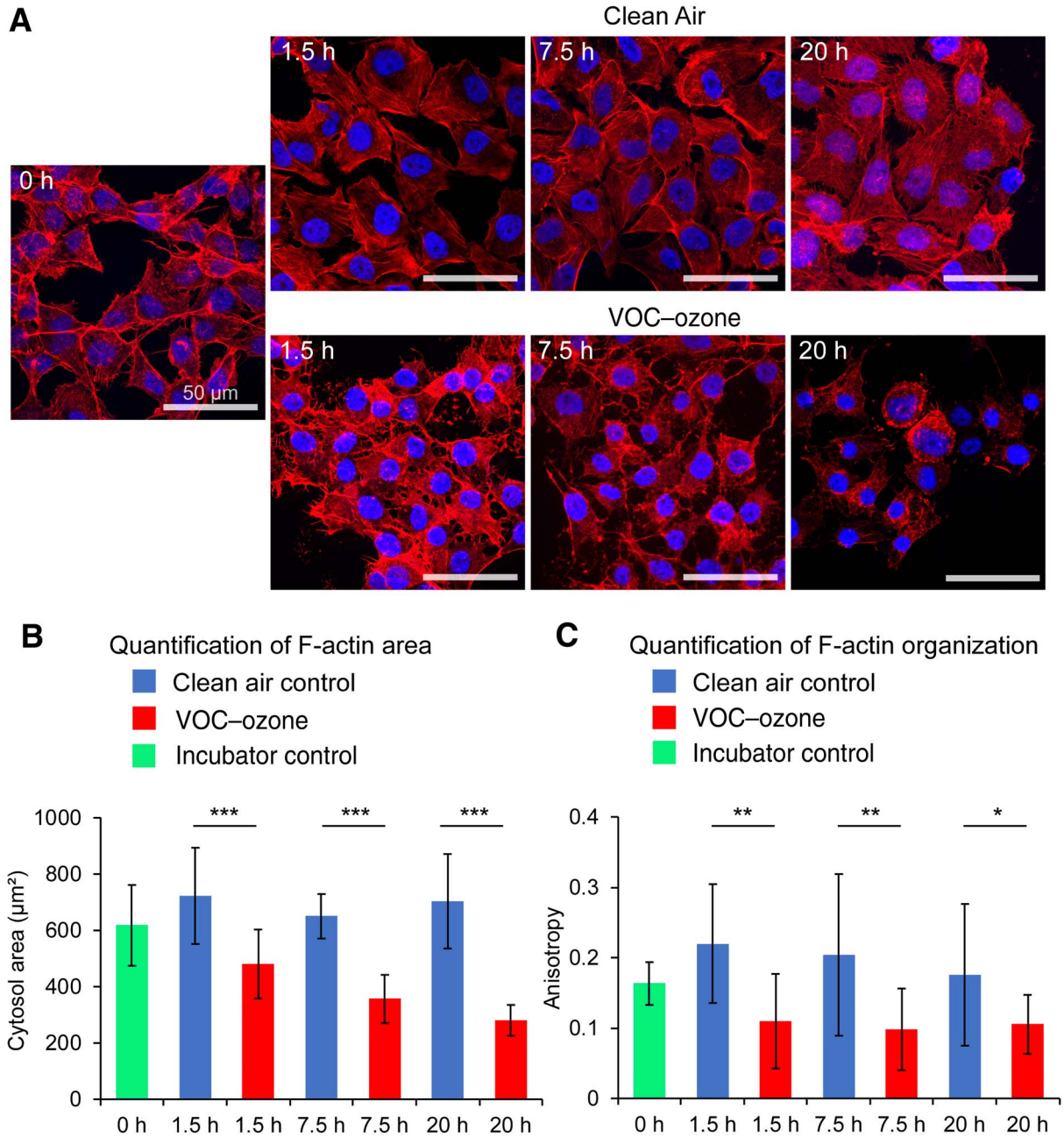

Figure 8. VOC–O_3 exposures inducing morphological changes and actin filament reorganization in BEAS-2B cells: (A) Confocal fluorescent microscopy of F-actin stained with Alexa Fluor 594 phalloidin and of nuclei stained with DAPI (magnification 63×). The images represent two independent air exposures. (Micrograph levels were adjusted to brighten, but not alter, image content.) **(B)** F-actin area, quantified using ImageJ; Twenty-five images were analyzed for each independent exposure. **(C)** Degree of anisotropy of actin fibril structures, quantified using the ImageJ plug-in FibrilTool. An anisotropy score of 0 indicates no order (purely isotropic fibrils); a score of 1 indicates perfectly parallel fibrils (purely anisotropic arrays). The analysis was conducted in 10 µm × 5 µm regions on 10 cells for each condition. Statistical analysis was computed by *t*-test analysis, and significance was denoted as * for P value < 0.05, ** for P value < 0.005, and *** for P value < 0.0005. (Portions of this figure from Gonzalez-Rivera et al. 2020. Figure 4, Panel D [Creative Commons Attribution 4.0 International License].)

unchanged in the clean air control, but cells had decreased F-actin area in the VOC–ozone mixtures at 7.5 hours. Furthermore, the difference in this area became significant in the VOC–ozone mixtures at 20 hours. In addition, we measured the degree of organization of the actin fibers in regions near the nucleus and the periphery of the cell using the FibrilTool app in Fiji/ImageJ (Figure 8C). The organization of actin fibers is an indicator of cytoskeleton activity and reorganization (Wilson and Gonzàles-Billault 2015). We found that the actin fibers were less organized in the VOC–ozone exposures compared with the clean air controls. In agreement with these observations, image analysis of the cell monolayer indicated a progressive loss of adherent BEAS-2B cells after exposure, with an accumulative loss of approximately 15% of the cells within 1.5 hours and of 60% of the cells within 20 hours (Additional Materials 1: Appendix A, Figure A.3).

To investigate the relationship between reduced expression and 8-oxoG enrichment after exposure, we selected the FDFT1 transcript from the list of downregulated genes that overlap with the list of 8-oxoG–enriched transcripts after exposure (Table). This transcript encodes a membrane-associated protein located at a branch point in the mevalonate pathway (Figure 9A). Because this gene regulates the first step in the cholesterol pathway, we evaluated the expression of FDFT1 protein by western blot analysis in cells exposed to VOC–ozone mixtures for 1.5 hours. The levels of FDFT1 protein decreased 60% in the exposed BEAS-2B compared with the clean air control (P value < 0.05) (Figure 9B). In addition, we hypothesized that the decrease in the levels of FDFT1 influenced the biosynthesis of cholesterol and would induce a decrease in the levels of cholesterol upon exposure. We conducted an analysis of cholesterol on whole cellular lysates of BEAS-2B cells exposed to VOC–ozone mixtures for 1.5 hours. Cholesterol decreased 29% in the exposed cells compared with the clean air control (P value < 0.05) (Figure 9C).

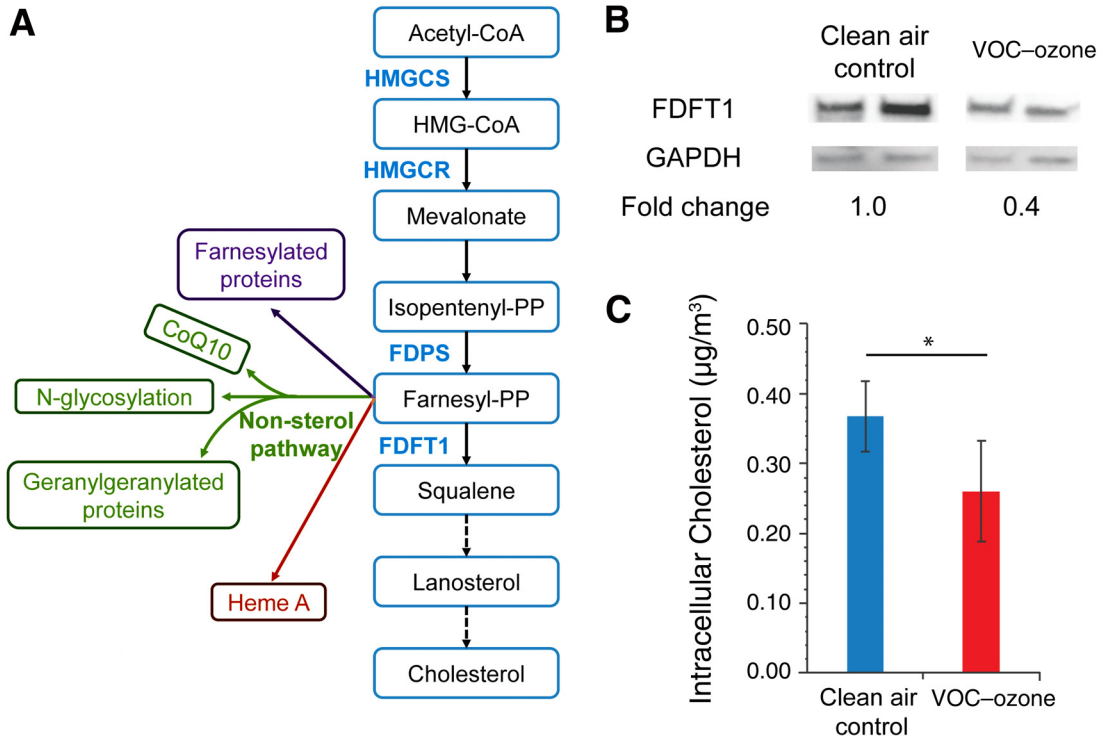

Figure 9. Changes induced by VOC–O_3 exposure in FDFT1 expression and cholesterol levels in BEAS-2B cells: (A) The mevalonate pathway leads to synthesis of cholesterol and various non-sterol isoprenoids. **(B)** Western blot analysis of FDFT1, a relevant biomarker associated with lipid biosynthesis, and GAPDH as control shows a decrease in the levels of protein expression when BEAS-2B cells were exposed to the VOC–O_3 mixture. Each band corresponds to an independent replicate. Fold changes were calculated by averaging the band's optical density for each condition. **(C)** Intracellular cholesterol levels were similarly affected, consistent with the downregulation of FDFT1 on exposure to the VOC–O_3 mixtures. Statistical analysis was computed by t-test analysis, and significance was denoted as * for P value < 0.05.

DISCUSSION, CONCLUSIONS, AND IMPLICATIONS

Oxidative stress has been demonstrated to be involved in the pathogenesis of COPD, asthma, pulmonary fibrosis, and lung cancer (Holguin 2013; Park et al. 2009) and to induce oxidative modifications in nucleic acids of mice and humans exposed to cigarette smoke and environmental benzene (Andreoli et al. 2015; Deslee et al. 2010). In the current study, we sought to investigate the effect of pro-oxidant air on alterations in the morphological and structural properties of BEAS-2B cells via oxidative modifications to relevant mRNAs in these pathways. Changes in these features are known to contribute to adverse health effects and can therefore serve as useful early biomarkers of air-induced oxidative stress in the lung. Pro-oxidant air was represented by VOC–ozone mixtures derived from 790 ppb ACR, 670 ppb MACR, and 4 ppm ozone. Our exposure conditions were expected to overwhelm cellular defenses and to show a linear response in 8-oxoG levels (Baldridge et al. 2015). Overall, the cells were exposed to a mixture of unreacted ACR and MACR, ozone, and VOC–ozone reaction products. It is possible that other components could have been introduced along with the volatilization of ACR and MACR. Hydroquinone, for example, is used as a stabilizer in ACR solutions, at concentrations between 0.25% and 0.35%. However, considering these low concentrations it is unlikely that the hydroquinone negatively affected the cell lines, given that we previously demonstrated that exposure to unreacted ACR and MACR (i.e., in the absence of ozone) caused no distinguishable cellular damage (as measured by LDH) in A549 cells compared with the clean air control cells (Baldridge et al. 2015). In this way, our studies suggest that the presence of small levels of hydroquinone or other contaminant compounds is not likely to have contributed to the cellular effects seen in the BEAS-2B cells.

The VOC precursors used in the current study are typically found in urban atmospheres. ACR and MACR are emitted in combustion processes and products, including tobacco smoke, cooking fumes, forest fires, and diesel combustion (Finlayson-Pitts and Pitts 1997; Stevens and Maier 2008). In addition, ozone is an atmospheric oxidant abundant in indoor and outdoor environments (Imlay and Linn 1988). Our physicochemical characterization of the VOC–ozone reaction mixture revealed that it contained products typical of moderately polluted atmospheres in some megacities (Cheng et al. 2016; Pant et al. 2017), during wildfire periods in urban areas of California (Wegesser et al. 2009), or while in traffic during confinement (i.e., between two large buildings) in any major U.S. city (Apte et al. 2017).

One important feature of our experimental setup was the use of an ALI system. Compared with the more frequently used submerged exposures that aim to assess the genotoxic effects of airborne pollutants (as summarized in Additional Materials 3: Appendix C, on the HEI website at *www.healtheffects.org/publications*), ALI systems allow more realistic exposure conditions. It is worth recalling that in vivo interactions with airborne substances occur at the boundary between ambient air and the epithelial layer in the airways. ALI systems also offer additional advantages over submerged exposures, in that they allow gas and particle phases to retain their intrinsic properties, thereby giving better control over effective doses (Latvala et al. 2016). In addition, ALI systems allow for gaseous air pollutant exposures and cell conditions that more realistically reflect in vivo organs (depending on the cell type, they allow formation of tight junctions, production of mucus, and cell differentiation). Furthermore, when directly compared, less variability in biomarker outcomes and higher sensitivity has been reported for ALI exposures than for submerged exposures (Upadhyay and Palmberg 2018). Some of the challenges of the ALI system, however, are efficient control of particle deposition (because of the formation of multiple layers instead of a monolayer) and conducting chronic-exposure studies (because of the limited cell lifetimes) (Paur et al. 2011).

In the current study, we first characterized our model system and demonstrated cellular responses in the levels of RNA oxidation (free 8-oxoG ribonucleotides) and cellular damage (LDH) after exposure. We observed higher levels of cellular damage (measured as LDH release) after exposure to the VOC–ozone mixtures compared with controls in the BEAS-2B cells than in our previous study in A549 cells using a similar VOC–ozone mixture. Given that most cancerous cells exhibit increased oxidative stress (Trachootham et al. 2009), we expect that this difference was caused by the higher tolerance of A549 cells to the pro-oxidant air. Alternatively, differences in cell types (alveolar cells in contrast to bronchial cells) that can be exposed to various oxygen and air pollutant tensions in the airways may partially account for the differing cellular responses to oxidative stress. Differences in culture media can also affect cellular responses, as suggested by Zhao and Klimecki (2015). In both the current study with BEAS-2B cells and our previous study with A549 cells, we followed the cell supplier's media-composition recommendations to ensure that the cells maintained the viability, genotype, and epigenotype of the reference cell line.

We detected accumulation of RNA oxidation in our BEAS-2B cells exposed to VOC–ozone mixtures, providing

evidence that the air composition generated by the VOC–ozone mixtures induced oxidative stress that led to chemical alterations in the structures of nucleobases such as 8-oxoG. This oxidative modification of the guanosine bases has been the most notable base oxidation in RNA with respect to alterations in genetic information (Dai et al. 2018). We used ELISA for detection of 8-oxoG, given that this assay is well established and has been used in stress studies and clinical analysis of nucleic acid oxidation (Shimoi et al. 2002; Toyokuni et al. 1997). Moreover, detection of this modification offers good sensitivity and selectivity, and it is relatively inexpensive. The strengths and limitations of immunoassays compared with mass spectrometry techniques have been extensively discussed elsewhere (Cross and Hornshaw 2016; Denburg et al. 2016; Hintze et al. 2011).

Clinically, 8-oxoG modification of RNAs is relevant in early neurodegeneration processes (Nunomura et al. 2001) and in severe COPD conditions (Deslee et al. 2010). Furthermore, detection of 8-oxoG is widely used in epidemiological studies as a biomarker for air pollution exposure and disease (Andreoli et al. 2015; Cejvanovic et al. 2018). Our findings suggest that relevant atmospheric agents influence the incidence of mRNA oxidation in lung cells that affect important phenotypic cellular properties, such as those reflected by cholesterol accumulation and cytoskeleton integrity. These studies highlight the importance of conducting additional mechanistic studies to connect the detrimental effects of environmental-related RNA oxidation with cellular functions.

Furthermore, we detected an expected high level of basal RNA oxidation in the clean air controls. To prevent artificial oxidation of the RNA by dissolved O_2 in solutions, we conducted all the steps in the RNA extraction, purification, and free 8-oxoG ELISA using freshly purged solutions with ultra-pure N_2. Even in the absence of an exogenous oxidative stress, natural cellular processes generate ROS that may not pose a functional burden to the cell. Although some level of basal RNA oxidation is expected and could play a functional role in the levels of epitranscriptomics marks (Fleming et al. 2017), this specific phenomenon requires further investigation.

Our transcriptomics and 8-oxoG RNA-Seq analysis of BEAS-2B cells exposed to VOC–ozone mixtures allowed us to identify 266 differentially expressed transcripts and 222 oxidized transcripts upon exposure. The functional analysis of these gene sets revealed a potential mechanism of cellular response to air pollution that is altered by a combination of changes in gene expression and incidence of specific transcript oxidation. One of the most interesting observations from the upregulated genes was the enrichment of the nanoparticle-mediated activation of the receptor signal pathway. This pathway is constituted by two transmembrane protein receptors, EGFR and integrin (Rauch et al. 2013). Transcripts associated with the former receptor were highly enriched in oxidized transcripts (Figure 7). The activation of EGFR is important in lung pathogenesis (Brambilla and Gazdar 2009; N'Guessan et al. 2014), and several respiratory studies have demonstrated that EGFR performs an essential function in signal transduction from a variety of atmospheric pollutants, including $PM_{2.5}$, cigarette smoke, and ozone (Feng et al. 2016; Filosto et al. 2012; Rumelhard et al. 2007). Aberrant activation of EGFR signaling by ROS is implicated in the development of lung cancer; it occurs via interaction with the c-Src tyrosine kinase (Filosto et al. 2012). Our studies indicated that multiple downstream signaling transcripts in the EGFR pathway are susceptible to RNA oxidation, perhaps suggesting that the abnormal activation of EGFR can be mediated by RNA adducts during oxidative stress. Furthermore, we observed differential upregulation of the transcript encoding c-Src. This protein triggers signaling networks in epithelial cells that induce cellular phenotypes identified in our study as being sensitive to RNA oxidation, such as apoptosis and inflammation via the first apoptotic signal (FAS) pathway (Rauch et al. 2013). It is worth noting that despite the upregulation of some genes associated with cell death, such as caspase 10 and hypoxia-inducible factor 1 alpha (Table B.1 in Additional Materials 2: Appendix B, on the HEI website at *www.healtheffects.org/publications*), our functional analysis indicated an enrichment of apoptosis-related genes in the downregulated gene list (Figure 6 and Table B.2 in Appendix B).

In addition to alterations in signaling pathways, the 8-oxoG RNA-Seq approach revealed that oxidative modifications induced by the VOC–ozone mixtures targeted transcripts associated with cytoskeleton actin filaments. These filaments mediate both biochemical and mechanical signals from and to the cellular environment and provide structural support to the cell. Abnormal organization of actin filaments is induced by environmental agents such as ozone and $PM_{2.5}$ (Thevenot et al. 2013; Yu et al. 1994) underlying a variety of respiratory conditions, such as cancer metastasis and lung fibrosis (Stueckle et al. 2018; Veljkovic et al. 2011). However, the link between the misregulation of cytoskeleton function and environmental factors is still unclear. Our study provides evidence that actin beta, one of the six transcripts encoding actin proteins, is targeted by RNA oxidation. Furthermore, major proteins controlling actin polymerization, depolymerization, and organization are encoded by transcripts highly enriched in RNA oxidation, such as the actin-related protein-2/3

complex, adenylyl cyclase-associated protein 1, cofilin, and LIM domain and actin-binding protein 1. Consequently, we evaluated the misregulation of cytoskeleton dynamics by confocal microscopy, confirming actin filament disorganization and a decrease in the extent of actin filaments. Importantly, similar alterations in the actin cytoskeleton were observed in BEAS-2B cells exposed to non-cytotoxic levels of formaldehyde (1 ppm) (Additional Materials 1: Appendix A, Figure A.5), indicating that alterations in cytoskeleton and cell shape occur independently of cytotoxicity responses generated by our mixture of air pollutants. In addition, consistent with current literature, BEAS-2B cells exposed to 50 μg/mL of urban $PM_{2.5}$ (Longhin et al. 2016) and to 20 μg/cm^2 radical-containing ultrafine PM (Thevenot et al. 2013) had alterations in cytoskeleton properties. To demonstrate loss of cytoskeleton integrity, we quantified the organization of phalloidin-stained F-actin microfilaments acquired by confocal microscopy. Our findings suggested that after exposure to VOC-ozone cells were unable to revert to the normal cytoskeleton arrangement after 20 hours of incubation, indicating a disruption of the cellular functions linked to microfilament polymerization and regulation. This result is consistent with previous studies demonstrating that polymerization of actin filaments is inhibited by a highly oxidative environment (Dalle-Donne et al. 2003). Collectively, our findings illustrate that dysfunction of the cytoskeleton caused by atmospheric factors is mediated by RNA oxidation, specifically targeting both actin-protein transcripts and actin-regulator transcripts.

Importantly, we found eight oxidized transcripts that were also downregulated by exposure to VOC–ozone. Of these, receptor-type tyrosine-protein phosphatase kappa, FDFT1, and prelamin-A/C are associated with either the plasma membrane or the cytoskeleton. One of the most interesting transcripts is FDFT1, which catalyzes the conversion of farnesyl pyrophosphate to squalene in the first step of the cholesterol biosynthesis pathway. Both cholesterol and cholesterol homeostasis genes have been implicated in cancer development and metastasis (Kuzu et al. 2016; Yang et al. 2014). We observed that the FDFT1 transcript was significantly enriched in 8-oxoG upon exposure, perhaps suggesting that selective oxidation of FDFT1 transcripts in air pollution exposures can disrupt FDFT1 regulation. Interestingly, the transcript that was identified in our approach is thought to undergo nonsense-mediated decay, one of the RNA-quality-control processes that relies on the recognition of abnormal RNA by the ribosome (Simms and Zaher 2016). We studied the expression of FDFT1 at the protein level and confirmed that downregulation of FDFT1 is associated with a decrease in the synthesis of cholesterol. Collectively, these results suggest that accumulation of 8-oxoG in certain transcripts, at least in the case of FDFT1, may disrupt gene regulation or alternative splicing patterns, ultimately leading to compromised function and disease.

Taken together, these findings demonstrate the influence of selective RNA oxidation by pro-oxidant environments in key cellular functions associated with stress signaling and the regulation of stress responses implicated in diseases. The strength of combining traditional transcriptome analysis with transcriptome-wide 8-oxoG mapping facilitated the discovery of detrimental effects on physiological pathways not characterized by current toxicogenomic approaches and has opened new avenues of research to more fully understand the adverse effects of air pollution on the physiological state of cells and their relationships with health conditions. Further studies are needed, particularly of exposures at lower non-cytotoxic concentrations, in order to more fully interpret the effects of the air pollutants examined at acute doses in our study and to conduct exposures with other pollutants (such as formaldehyde) to facilitate comparison with other substances known to react with nucleic acids (Tanaka et al. 2011).

ACKNOWLEDGMENTS

We would like to thank all members of Dr. Contreras's laboratory for discussions, suggestions and support. We thank P. Reena Bhikha (University of Texas, Austin, McKetta Dept. of Chemical Engineering) and Katherine O'Connor (University of Texas, Austin, Department of Biomedical Engineering) for their assistance with cell cultures and biochemical assays. RNA library preparation and sequencing were conducted in the Genomic Sequencing and Analysis Facility of the Center for Biomedical Research Support at The University of Texas at Austin in consultation with Jessica Podnar. The quantitative label-free proteomics analysis was performed in the Proteomics Facility of the Center for Biomedical Research Support at The University of Texas at Austin in consultation with Dr. Maria Person. We thank The Texas Advanced Computing Center (TACC) at The University of Texas, Austin, for providing high-performance computing resources, and the Microscopy and Imaging Facility of the Center for Biomedical Research Support at The University of Texas, Austin, for providing the confocal microscope. J.C.G-R. was supported by Administrative Department of Science, Technology, and Innovation (COLCIENCIAS) of Colombia and Fulbright (Grant 479) and K.C.B. was supported by National Defense Science and Engineering Graduate Fellowship (NDSEG) program.

REFERENCES

Aljawhary D, Lee AKY, Abbatt JPD. 2013. High-resolution chemical ionization mass spectrometry (ToF-CIMS): Application to study SOA composition and processing. Atmos Meas Tech 6(11):3211–3224.

Allan JD, Delia AE, Coe H, Bower KN, Alfarra MR, Jimenez JL, et al. 2004. A generalised method for the extraction of chemically resolved mass spectra from aerodyne aerosol mass spectrometer data. J Aerosol Sci 35:909–922.

Almogbel E, Rasheed N. 2017. Protein mediated oxidative stress in patients with diabetes and its associated neuropathy: Correlation with protein carbonylation and disease activity markers. J Clin Diag Res 11:BC21–BC25.

Andreoli R, Spatari G, Pigini D, Poli D, Banda I, Goldoni M, et al. 2015. Urinary biomarkers of exposure and of oxidative damage in children exposed to low airborne concentrations of benzene. Environ Res 142:264–272.

Apte JS, Messier KP, Gani S, Brauer M, Kirchstetter TW, Lunden MM, et al. 2017. High-resolution air pollution mapping with Google Street View cars: Exploiting big data. Environ Sci Tech 51:6999–7008.

Baldridge KC, Zavala J, Surratt J, Sexton KG, Contreras LM. 2015. Cellular RNA is chemically modified by exposure to air pollution mixtures. Inhal Toxicol 27:74–82.

Barker TH, Dysart MM, Brown AC, Douglas AM, Fiore VF, Russell AG, et al. 2014. Synergistic Effects of Particulate Matter and Substrate Stiffness on Epithelial-to-Mesenchymal Transition. Research Report 182. Boston, MA: Health Effects Institute.

Barrera G. 2012. Oxidative stress and lipid peroxidation products in cancer progression and therapy. ISRN Oncology 2012:137289.

Boudaoud A, Burian A, Borowska-Wykret D, Uyttewaal M, Wrzalik R, Kwiatkowska D, et al. 2014. FibrilTool, an ImageJ plug-in to quantify fibrillar structures in raw microscopy images. Nat Protoc 9:457–463.

Brambilla E, Gazdar A. 2009. Pathogenesis of lung cancer signalling pathways: Roadmap for therapies. Eur Respir J 33:1485–1497.

Budisulistiorini SH, Canagaratna MR, Croteau PL, Marth WJ, Baumann K, Edgerton ES, et al. 2013. Real-time continuous characterization of secondary organic aerosol derived from isoprene epoxydiols in downtown Atlanta, Georgia, using the aerodyne aerosol chemical speciation monitor. Environ Sci Tech 47:5686–5694.

Calabretta A, Kupfer PA, Leumann CJ. 2015. The effect of RNA base lesions on mRNA translation. Nucleic Acids Res 43:4713–4720.

Canagaratna MR, Jayne JT, Jimenez JL, Allan JD, Alfarra MR, Zhang Q, et al. 2007. Chemical and microphysical characterization of ambient aerosols with the aerodyne aerosol mass spectrometer. Mass Spectrom Rev 26:185–222.

Castro JP, Jung T, Grune T, Siems W. 2017. 4-Hydroxynonenal (HNE) modified proteins in metabolic diseases. Free Radic Biol Med 111:309–315.

Cejvanovic V, Kjaer LK, Mørup Bergholdt HK, Henriksen T, Weimann A, Ellervik C, et al. 2018. RNA oxidation and iron levels in patients with diabetes. Free Radic Biol Med 129:532–536.

Chadwick AC, Holme RL, Chen Y, Thomas MJ, Sorci-Thomas MG, Silverstein RL, et al. 2015. Acrolein impairs the cholesterol transport functions of high density lipoproteins. PloS One 10(4):e0123138.

Chen C, Arjomandi M, Balmes J, Tager I, Holland N. 2007. Effects of chronic and acute ozone exposure on lipid peroxidation and antioxidant capacity in healthy young adults. Environ Health Perspect 115:1732–1737.

Chen EY, Tan CM, Kou Y, Duan Q, Wang Z, Meirelles GV, et al. 2013. Enrichr: Interactive and collaborative HTML5 gene list enrichment analysis tool. BMC Bioinformatics 14:128.

Cheng TJ, Kao HP, Chan CC, Chang WP. 2003. Effects of ozone on DNA single-strand breaks and 8-oxoguanine formation in A549 cells. Environ Res 93:279–284.

Cheng Y, Zheng G, Wei C, Mu Q, Zheng B, Wang Z, et al. 2016. Reactive nitrogen chemistry in aerosol water as a source of sulfate during haze events in China. Sci Adv 2(12): e1601530.

Cho HY, Morgan DL, Bauer AK, Kleeberger SR. 2007. Signal transduction pathways of tumor necrosis factor-mediated lung injury induced by ozone in mice. Amer J Respir Crit Care Med 175:829–839.

Cohen AJ, Brauer M, Burnett R, Anderson HR, Frostad J, Estep K, et al. 2017. Estimates and 25-year trends of the global burden of disease attributable to ambient air pollution: An analysis of data from the Global Burden of Diseases Study 2015. Lancet 389:1907–1918.

Conklin DJ. 2016. Acute cardiopulmonary toxicity of inhaled aldehydes: Role of TRPA1. Ann N Y Acad Sci 1374:59–67.

Conklin DJ, Barski OA, Lesgards JF, Juvan P, Rezen T, Rozman D, et al. 2010. Acrolein consumption induces systemic dyslipidemia and lipoprotein modification. Toxicol Appl Pharmacol 243:1–12.

Cooke MS, Evans MD, Dizdaroglu M, Lunec J. 2003. Oxidative DNA damage: Mechanisms, mutation, and disease. FASEBJ 17:1195–1214.

Cross TG, Hornshaw MP. 2016. Can LC and LC-MS ever replace immunoassays? J Appl Bionalysis 2:108.

Dai DP, Gan W, Hayakawa H, Zhu JL, Zhang XQ, Hu GX, et al. 2018. Transcriptional mutagenesis mediated by 8-oxoG induces translational errors in mammalian cells. Proc Natl Acad Sci U S A 115:4218–4222.

Dalle-Donne I, Giustarini D, Rossi R, Colombo R, Milzani A. 2003. Reversible S-glutathionylation of Cys 374 regulates actin filament formation by inducing structural changes in the actin molecule. Free Radic Biol Med 34:23–32.

Davies MJ. 2016. Protein oxidation and peroxidation. Biochem J 473:805–825.

Del Rio D, Stewart AJ, Pellegrini N. 2005. A review of recent studies on malondialdehyde as toxic molecule and biological marker of oxidative stress. Nutr Metab Cardiovasc Dis 15:316–328.

Denburg MR, Hoofnagle AN, Sayed S, Gupta J, de Boer IH, Appel LJ, et al. 2016. Comparison of two ELISA methods and mass spectrometry for measurement of vitamin D-binding protein: Implications for the assessment of bioavailable vitamin D concentrations across genotypes. J Bone Miner Res 31:1128–1136.

Deslee G, Adair-Kirk TL, Betsuyaku T, Woods JC, Moore CH, Gierada DS, et al. 2010. Cigarette smoke induces nucleic-acid oxidation in lung fibroblasts. Amer J Respir Cell Mol Biol 43:576–584.

Dominissini D, Moshitch-Moshkovitz S, Salmon-Divon M, Amariglio N, Rechavi G. 2013. Transcriptome-wide mapping of N(6)-methyladenosine by m(6) A-seq based on immunocapturing and massively parallel sequencing. Nat Protoc 8:176–189.

Dorado-Martinez C, Paredes-Carbajal C, Mascher D, Borgonio-Pérez G, Rivas-Arancibia S. 2001. Effects of different ozone doses on memory, motor activity and lipid peroxidation levels, in rats. Int J Neurosci 108:149–161.

Doyle M, Sexton KG, Jeffries H, Jaspers I. 2007. Atmospheric photochemical transformations enhance 1,3-butadiene-induced inflammatory responses in human epithelial cells: The role of ozone and other photochemical degradation products. Chem Biol Interact 166:163–169.

Faroon O, Roney N, Taylor J, Ashizawa A, Lumpkin MH, Plewak DJ. 2008. Acrolein health effects. Toxicol Ind Health 24:447–490.

Feng F, Jin Y, Duan L, Yan Z, Wang S, Li F, et al. 2016. Regulation of ozone-induced lung inflammation by the epidermal growth factor receptor in mice. Environ Toxicol 31:2016–2027.

Filosto S, Becker CR, Goldkorn T. 2012. Cigarette smoke induces aberrant EGF receptor activation that mediates lung cancer development and resistance to tyrosine kinase inhibitors. Mol Cancer Ther 11:795–804.

Finlayson-Pitts BJ, Pitts JN Jr. 1997. Tropospheric air pollution: Ozone, airborne toxics, polycyclic aromatic hydrocarbons, and particles. Science 276:1045–1052.

Fleming AM, Ding Y, Burrows CJ. 2017. Oxidative DNA damage is epigenetic by regulating gene transcription via base excision repair. Proc Natl Acad Sci U S A 114:2604–2609.

Gonzalez-Rivera JC, Baldridge KC, Wang DS, Patel K, Chuvalo-Abraham JCL, Ruiz LH, et al. 2020. Post-transcriptional air pollution oxidation to the cholesterol biosynthesis pathway promotes pulmonary stress phenotypes. Commun Biol 3 (392); https://doi.org/10.1038/s42003-020-01118-6.

Graham RM, Friedman M, Hoyle GW. 2001. Sensory nerves promote ozone-induced lung inflammation in mice. Amer J Respir Crit Care Med164:307–313.

Henning RJ, Johnson GT, Coyle JP, Harbison RD. 2017. Acrolein can cause cardiovascular disease: A review. Cardiovasc Toxicol 17:227–236.

Hintze JP, Tomatsu S, Fujii T, Montano AM, Yamaguchi S, Suzuki Y, et al. 2011. Comparison of liquid chromatography-tandem mass spectrometry and sandwich ELISA for determination of keratan sulfate in plasma and urine. Biomark Insights 6:69–78.

Hohn A, Konig J, Grune T. 2013. Protein oxidation in aging and the removal of oxidized proteins. J Proteomics 92:132–159.

Holguin F. 2013. Oxidative stress in airway diseases. Ann Am Thorac Soc 10 Suppl:S150–157.

Huang Y, Zhao R, Charan SM, Kenseth CM, Zhang X, Seinfeld JH. 2018. Unified theory of vapor-wall mass transport in teflon-walled environmental chambers. Environ Sci Technol 52:2134–2142.

Imlay JA, Linn S. 1988. DNA damage and oxygen radical toxicity. Science 240:1302–1309.

Kampf CJ, Liu F, Reinmuth-Selzle K, Berkemeier T, Meusel H, Shiraiwa M, et al. 2015. Protein cross-linking and oligomerization through dityrosine formation upon exposure to ozone. Environ Sci Technol 49:10859–10866.

Kehrer JP, Biswal SS. 2000. The molecular effects of acrolein. Toxicol Sci 57:6–15.

Kuleshov MV, Jones MR, Rouillard AD, Fernandez NF, Duan Q, Wang Z, et al. 2016. Enrichr: A comprehensive gene set enrichment analysis web server 2016 update. Nucleic Acids Res 44:W90-97.

Kuzu OF, Noory MA, Robertson GP. 2016. The role of cholesterol in cancer. Cancer Res 76:2063–2070.

Lai CH, Lee CN, Bai KJ, Yang YL, Chuang KJ, Wu SM, et al. 2016. Protein oxidation and degradation caused by particulate matter. Sci Rep 6:33727.

Latvala S, Hedberg J, Möller L, Odnevall Wallinder I, Karlsson HL, Elihn K. 2016. Optimization of an air-liquid interface exposure system for assessing toxicity of airborne nanoparticles. J Appl Toxicol 36:1294–1301.

Li H, Wang J, Kaphalia B, Ansari GA, Khan MF. 2004. Quantitation of acrolein-protein adducts: Potential biomarker of acrolein exposure. J Toxicol Environ Health Part A 67:513–524.

Li L, Jiang L, Geng C, Cao J, Zhong L. 2008. The role of oxidative stress in acrolein-induced DNA damage in HepG2 cells. Free Radic Res 42:354–361.

Li X, Xiong X, Yi C. 2016. Epitranscriptome sequencing technologies: Decoding RNA modifications. Nat Methods 14:23–31.

Li Z, Malla S, Shin B, Li JM. 2014. Battle against RNA oxidation: Molecular mechanisms for reducing oxidized RNA to protect cells. Wiley Interdiscip Rev RNA 5:335–346.

Liang X, Liu L, Fu T, Zhou Q, Zhou D, Xiao L, et al. 2016. Exercise inducible lactate dehydrogenase B regulates mitochondrial function in skeletal muscle. J Biol Chem 291:25306–25318.

Longhin E, Capasso L, Battaglia C, Proverbio MC, Cosentino C, Cifola I, et al. 2016. Integrative transcriptomic and protein analysis of human bronchial BEAS-2B exposed to seasonal urban particulate matter. Environ Pollut 209:87–98.

Love MI, Huber W, Anders S. 2014. Moderated estimation of fold change and dispersion for RNA-seq data with DESeq2. Genome Biol 15:550.

McHale CM, Zhang L, Hubbard AE, Smith MT. 2010. Toxicogenomic profiling of chemically exposed humans in risk assessment. Mutat Res 705:172–183.

Moghe A, Ghare S, Lamoreau B, Mohammad M, Barve S, McClain C, et al. 2015. Molecular mechanisms of acrolein toxicity: Relevance to human disease. Toxicol Sci 143: 242–255.

Nah T, McVay RC, Pierce JR, Seinfeld JH, Ng NL. 2017. Constraining uncertainties in particle-wall deposition correction during SOA formation in chamber experiments. Atmos Chem Phys 17:2297–2310.

Nehls P, Seiler F, Rehn B, Greferath R, Bruch J. 1997. Formation and persistence of 8-oxoguanine in rat lung cells as an important determinant for tumor formation following particle exposure. Environ Health Perspect 105 Suppl 5:1291–1296.

Ng NL, Canagaratna MR, Jimenez JL, Chhabra PS, Seinfeld JH, Worsnop DR. 2011. Changes in organic aerosol composition with aging inferred from aerosol mass spectra. Atmos Chem Phys 11:6465–6474.

N'Guessan PD, Haarmann H, Steiner T, Heyl K, Schreiber F, Heinrich A, et al. 2014. The moraxella catarrhalis-induced pro-inflammatory immune response is enhanced by the activation of the epidermal growth factor receptor in human pulmonary epithelial cells. Biochem Biophys Res Commun 450:1038–1044.

Nunomura A, Castellani RJ, Zhu X, Moreira PI, Perry G, Smith MA. 2006. Involvement of oxidative stress in Alzheimer disease. J Neuropathol Exp Neurol 65:631–641.

Nunomura A, Moreira PI, Castellani RJ, Lee HG, Zhu X, Smith MA, et al. 2012. Oxidative damage to RNA in aging and neurodegenerative disorders. Neurotox Res 22:231–248.

Nunomura A, Perry G, Aliev G, Hirai K, Takeda A, Balraj EK, et al. 2001. Oxidative damage is the earliest event in Alzheimer disease. J Neuropathol Exp Neurol 60:759–767.

Pant P, Habib G, Marshall JD, Peltier RE. 2017. $PM_{2.5}$ exposure in highly polluted cities: A case study from New Delhi, India. Environ Res 156:167–174.

Park HS, Kim SR, Lee YC. 2009. Impact of oxidative stress on lung diseases. Respirology 14:27–38.

Paur H-R, Cassee FR, Teeguarden J, Fissan H, Diabate S, Aufderheide M, et al. 2011. In-vitro cell exposure studies for the assessment of nanoparticle toxicity in the lung—A dialog between aerosol science and biology. J Aerosol Sci 42:668–692.

Rager JE, Smeester L, Jaspers I, Sexton KG, Fry RC. 2011. Epigenetic changes induced by air toxics: Formaldehyde exposure alters miRNA expression profiles in human lung cells. Environ Health Perspect 119:494–500.

Rauch J, Kolch W, Laurent S, Mahmoudi M. 2013. Big signals from small particles: Regulation of cell signaling pathways by nanoparticles. Chem Rev 113:3391–3406.

Ren Y, Grosselin B, Daele V, Mellouki A. 2017. Investigation of the reaction of ozone with isoprene, methacrolein and methyl vinyl ketone using the HELIOS chamber. Faraday Discuss 200:289–311.

Rivas-Arancibia S, Guevara-Guzmán R, López-Vidal Y, Rodriguez-Martinez E, Zanardo-Gomes M, Angoa-Pérez M, et al. 2010. Oxidative stress caused by ozone exposure induces loss of brain repair in the hippocampus of adult rats. Toxicol Sci 113:187–197.

Rivas-Arancibia S, Zimbrón LF, Rodriguez-Martinez E, Maldonado PD, Borgonio Pérez G, Sepúlveda-Parada M. 2015. Oxidative stress-dependent changes in immune responses and cell death in the substantia nigra after ozone exposure in rat. Front Aging Neurosci 7:65.

Rumelhard M, Ramgolam K, Hamel R, Marano F, Baeza-Squiban A. 2007. Expression and role of EGFR ligands induced in airway cells by PM2.5 and its components. Eur Respir J 30:1064–1073.

Schurch NJ, Schofield P, Gierlinski M, Cole C, Sherstnev A, Singh V, et al. 2016. How many biological replicates are needed in an RNA-seq experiment and which differential expression tool should you use? RNA 22:839–851.

Shan X, Lin CL. 2006. Quantification of oxidized RNAs in Alzheimer's disease. Neurobiol Aging 27:657–662.

Shan X, Tashiro H, Lin CL. 2003. The identification and characterization of oxidized RNAs in Alzheimer's disease. J Neurosci 23:4913–4921.

Shimoi K, Kasai H, Yokota N, Toyokuni S, Kinae N. 2002. Comparison between high-performance liquid chromatography and enzyme-linked immunosorbent assay for the determination of 8-hydroxy-2′-deoxyguanosine in human urine. Cancer Epidemiol Biomarkers Prev 11:767–770.

Simms CL, Zaher HS. 2016. Quality control of chemically damaged RNA. Cell Mol Life Sci 73:3639–3653.

Sousa SI, Alvim-Ferraz MC, Martins FG. 2013. Health effects of ozone focusing on childhood asthma: What is now known — A review from an epidemiological point of view. Chemosphere 90:2051–2058.

Stevens JF, Maier CS. 2008. Acrolein: Sources, metabolism, and biomolecular interactions relevant to human health and disease. Mol Nutr Food Res 52:7–25.

Stueckle TA, Davidson DC, Derk R, Kornberg TG, Battelli L, Friend S, et al. 2018. Short-term pulmonary toxicity assessment of pre- and post-incinerated organomodified nanoclay in mice. ACS Nano 12:2292–2310.

Takeuchi K, Kato M, Suzuki H, Akhand AA, Wu J, Hossain K, et al. 2001. Acrolein induces activation of the epidermal growth factor receptor of human keratinocytes for cell death. J Cell Biochem 81:679–688.

Tanaka M, Han S, Kupfer PA, Leumann CJ, Sonntag WE. 2011. An assay for RNA oxidation induced abasic sites using the aldehyde reactive probe. Free Radic Res 45:237–247.

Thevenot PT, Saravia J, Jin N, Giaimo JD, Chustz RE, Mahne S, et al. 2013. Radical-containing ultrafine particulate matter initiates epithelial-to-mesenchymal transitions in airway epithelial cells. Amer J Respir Cell Mol Biol 48:188–197.

Toyokuni S, Tanaka T, Hattori Y, Nishiyama Y, Yoshida A, Uchida K, et al. 1997. Quantitative immunohistochemical determination of 8-hydroxy-2'-deoxyguanosine by a monoclonal antibody N45.1: Its application to ferric nitrilotriacetate-induced renal carcinogenesis model. Lab Invest 76:365–374.

Trachootham D, Alexandre J, Huang P. 2009. Targeting cancer cells by ROS-mediated mechanisms: A radical therapeutic approach? Nat Rev Drug Discov 8:579–591.

Uhlen M, Zhang C, Lee S, Sjöstedt E, Fagerberg L, Bidkhori G, et al. 2017. A pathology atlas of the human cancer transcriptome. Science 357.

Upadhyay S, Palmberg L. 2018. Air-liquid interface: Relevant in vitro models for investigating air pollutant-induced pulmonary toxicity. Toxicol Sci 164:21–30.

Veljkovic E, Jiricny J, Menigatti M, Rehrauer H, Han W. 2011. Chronic exposure to cigarette smoke condensate in vitro induces epithelial to mesenchymal transition-like

changes in human bronchial epithelial cells, BEAS-2B. Toxicol In Vitro 25:446–453.

Wang JX, Gao J, Ding SL, Wang K, Jiao JQ, Wang Y, et al. 2015. Oxidative modification of miR-184 enables it to target Bcl-xl and Bcl-w. Mol Cell 59:50–61.

Wegesser TC, Pinkerton KE, Last JA. 2009. California wildfires of 2008: Coarse and fine particulate matter toxicity. Environ Health Perspect 117:893–897.

WHO (World Health Organization). 2018. Air pollution. Available: *www.who.int/airpollution/en/* [accessed 30 Jun 2018].

Wilson C, González-Billault C. 2015. Regulation of cytoskeletal dynamics by redox signaling and oxidative stress: Implications for neuronal development and trafficking. Front Cell Neurosci 9:381.

Yang YF, Jan YH, Liu YP, Yang CJ, Su CY, Chang YC, et al. 2014. Squalene synthase induces tumor necrosis factor receptor 1 enrichment in lipid rafts to promote lung cancer metastasis. Amer J Respir Crit Care Med 190:675–687.

Yu XY, Takahashi N, Croxton TL, Spannhake EW. 1994. Modulation of bronchial epithelial cell barrier function by in vitro ozone exposure. Environ Health Perspect 102:1068–1072.

Zhao F, Klimecki WT. 2015. Culture conditions profoundly impact phenotype in BEAS-2B, a human pulmonary epithelial model. J Appl Toxicol 35:945–951.

MATERIALS AVAILABLE ON THE HEI WEBSITE

Additional Materials 1–3 contain supplemental material (Appendices A, B, and C) not included in the printed report. They are available on the HEI Web site, *www.healtheffects.org/publications*.

Additional Materials 1: Appendix A. Supplementary Figures

Additional Materials 2: Appendix B. Tables of Differentially Expressed and Significantly Oxidized Transcripts upon Exposure and Tables from the Functional Enrichment Analysis

Additional Materials 3: Appendix C. Review of Toxicogenomic Studies of Exposed Models to Environmental Agents

ABOUT THE AUTHORS

Lydia M. Contreras, Ph.D., has been an associate professor since 2011 in the McKetta Department of Chemical Engineering of the University of Texas, Austin. She is also a member of the university's biophysics graduate program and its Institute for Cellular and Molecular Biology. She earned her BSE in chemical engineering in 2003 from Princeton University in Princeton, New Jersey, and her Ph.D. in 2008 from Cornell University in Ithaca, New York. As a graduate student, she developed a novel intracellular mRNA-protein display technology that has been patented and licensed by a company based in Ithaca. She conducts fundamental research in the areas of RNA-protein chemistry and the molecular characterization of ribonucleoprotein complexes.

Juan C. Gonzalez-Rivera, M.S., is a chemical engineering graduate research assistant seeking his Ph.D. in the laboratory of Dr. Lydia Contreras at the University of Texas, Austin. He earned his BSE in chemical engineering in 2011 and his M.S. in electronics engineering in 2014 from the University of Los Andes in Bogotá, Colombia, where his work focused on developing electrochemical biosensors embedded on microfluidic devices for applications in the biomedical industry. Currently, he is interested in understanding how environmental stresses can alter the molecular properties of RNA that can lead to detrimental effects in lung cells.

Kevin C. Baldridge, Ph.D., is a postdoctoral fellow in the laboratory of Dr. Daniel J. Leahy at the University of Texas, Austin. He earned his Ph.D. in chemical engineering from the University of Texas, Austin, where his work focused on how post-transcriptional and environmental RNA modifications play roles in cellular stress. He is currently studying EGFR family mutants relevant to cancer research.

Dongyu S. Wang, Ph.D., earned his Ph.D. in chemical engineering from the University of Texas, Austin, where his graduate studies focused on the formation and characterization of secondary organic aerosols in the atmosphere. In 2018, he joined the Paul Scherrer Institute in Villigen and Würenlingen, Switzerland, as a postdoctoral researcher to investigate particle nucleation and to develop novel detection techniques.

Jamie C. L. Chuvalo-Abraham is a chemical engineering undergraduate research assistant in the laboratory of Dr. Lydia Contreras at the University of Texas, Austin. Her current research focuses on examining the effects of air pollution on human health. After graduation, she plans to attend

law school to earn her J.D., with a focus on intellectual property law.

Lea Hildebrandt Ruiz, Ph.D., is an assistant professor in the McKetta Department of Chemical Engineering and at the Center for Energy and Environmental Resources at the University of Texas, Austin. Her research interests lie in atmospheric chemistry and the effects of physicochemical processing of pollutants on human exposure and health. She conducts research using state-of-the-science mass spectrometric instrumentation to conduct policy-relevant and fundamental chemical research and has been involved in the development and refinement of mass spectrometric techniques. She has participated in planning, conducting, and analyzing the results of several projects focused on laboratory chamber experiments and field campaigns in indoor and outdoor environments.

OTHER PUBLICATIONS RESULTING FROM THIS RESEARCH

Gonzalez-Rivera JC, Baldridge KC, Wang DS, Patel K, Chuvalo-Abraham JCL, Ruiz LH, et al. 2020. Post-transcriptional air pollution oxidation to the cholesterol biosynthesis pathway promotes pulmonary stress phenotypes. Commun Biol 3(392); https://doi.org/10.1038/s42003-020-01118-6.

Orr AA, Gonzalez-Rivera JC, Wilson M, Bhikha PR, Wang D, Contreras LM, Tamamis P. 2018. A high-throughput and rapid computational method for screening of RNA post-transcriptional modifications that can be recognized by target proteins. Methods 143:34–47.

Mihailovic MK, Chen A, Gonzalez-Rivera JC, Contreras LM. 2017. Defective ribonucleoproteins, mistakes in RNA processing, and diseases. Biochemistry 56:1367–1382.

CRITIQUE

Review Committee

HEI

Research Report 201, *Understanding the Functional Impact of VOC–Ozone Mixtures on the Chemistry of RNA in Epithelial Lung Cells*, L. M. Contreras et al.

INTRODUCTION

Ozone is a highly reactive gas that is a major component of air pollution. Exposure to ozone via inhalation affects the respiratory tract and the lungs, resulting in inflammation and changes in respiration. Effects on the cardiovascular system and other organs may also ensue (U.S. EPA 2013). Volatile organic compounds (VOCs*), such as the aldehydes acrolein and methacrolein, are also components of the air pollution mixture, especially in urban environments (Stevens and Maier 2008). Combustion of carbohydrates in biomass, food, and tobacco is a major source of acrolein, and oxidation of isoprene (emitted by trees, for example) is a major source of methacrolein. Inhaling acrolein or methacrolein induces irritation in the airways, via activation of airway neuroreceptors. VOCs can also react with ozone in the atmosphere to form secondary organic aerosols (Hallquist et al. 2009; Kroll and Seinfeld 2008), which constitute a component of ambient particulate matter that can in turn have deleterious effects on human health.

Exposure to either ozone or VOCs can damage multiple components inside cells of the respiratory tract, such as lipids, proteins, and DNA (Byvoet et al. 1995; Cataldo 2006). Few studies, however, have looked at the effects of exposure to ozone or VOCs on ribonucleic acid (RNA) inside cells. Cells contain over four times more RNA than DNA per unit mass, and multiple types of RNA play crucial roles inside cells. These include messenger RNA (mRNA) and transfer RNA, from which amino acids are made on ribosomes; ribosomal RNA, a key constituent of ribosome structure and function; and microRNAs (miRNAs), which have regulatory functions.

To begin to examine the effects of air pollutants on RNA, Dr. Lydia Contreras of the University of Texas, Austin, submitted an application to HEI titled "Understanding the impact of air quality on the changing chemistry of regulatory nucleic acids that affect human health" in response to HEI's Request for Applications 14-2, *Walter A. Rosenblith New Investigator Award*. This award was established to provide support for an outstanding new investigator at the assistant professor level to conduct research in the area of air pollution and health and is unrestricted with respect to the topic of research. Dr. Contreras proposed to investigate how exposure to urban air pollution mixtures might induce changes in different species of RNA, particularly mRNAs and regulatory miRNAs. In addition, she proposed to study how such changes in RNA chemistry might affect biological responses. HEI funded Contreras's application, considering it a new area worthy of study in understanding the mechanisms by which air pollutants might act.

This Critique provides the HEI Review Committee's independent evaluation of the study. It is intended to aid the sponsors of HEI and the public by highlighting both the strengths and limitations of the study and by placing the Investigators' Report into scientific and regulatory perspective.

SCIENTIFIC BACKGROUND

HEALTH EFFECTS OF OZONE AND VOCS

Ozone is a strong oxidant; in aqueous solutions it decomposes to produce reactive oxygen species (ROS), such as superoxide, hydroxy radicals, and hydrogen peroxide. In mammalian cells, these ROS are also generated endogenously as byproducts of adenosine triphosphate production and oxygen utilization. When the balance of antioxidants and pro-oxidants such as ROS tips toward pro-oxidants, oxidative stress results. Oxidative stress has been identified as a unifying feature of the pathophysiological responses to air pollutants that include ozone and particulate matter (Kelly 2003; Li et al. 2003).

The inhalation of reactive aldehydes such as acrolein and methacrolein activates receptors present on neurons innervating the airways, resulting in increased vascular permeability and leakage of leukocytes into the surrounding tissue. Activation also results in the release of neuropeptides

Dr. Lydia M. Contreras's 3-year study, "Understanding the impact of air quality on the changing chemistry of regulatory nucleic acids that affect human health," began in May 2015. Total expenditures were $395,333. The draft Investigators' Report from Contreras and colleagues was received for review in July 2018. A revised report, received in January 2019, was accepted for publication in February 2019. During the review process, the HEI Review Committee and the investigators had the opportunity to exchange comments and to clarify issues in both the Investigators' Report and the Review Committee's Critique.

* A list of abbreviations and other terms appears at the end of this volume.

such as substance P, neurokinin A, and calcitonin gene-related peptide, which mediate bronchoconstriction and leakage of plasma proteins into the airways.

DNA AND RNA OXIDATION

DNA Oxidation

Oxidation reactions that involve ROS inside cells generate several types of damage to DNA (Cadet et al. 2002). These include purine and pyrimidine base lesions, oligonucleotide strand breaks, the generation of abasic sites, and DNA–protein cross-links. In addition, reactive aldehydes can react with DNA to form adducts via Michael additions, in which they add a carbon atom to the structure. Formation of these adducts constitutes another class of oxidative damage to DNA.

Because guanine is more easily oxidized than the other nucleosides, 8-hydroxy-2′-deoxyguanosine (8-OH-dG) is a major product of DNA oxidation. It is a biomarker of oxidative stress, and high levels of 8-OH-dG have been associated with the induction of carcinogenesis (Cooke et al. 2008).

RNA Oxidation

Oxidation of RNA has been much less studied than the oxidation of DNA, but reactions similar to those of ROS with DNA have been described. Thus, oxidation of individual RNA bases guanine, cytosine, adenine, and uracil has been detected (Nunomura et al. 2017). As in DNA, guanine in RNA is particularly sensitive to oxidation, resulting in the product 8-oxo-7,8-dihydroguanine (8-oxoG). It is also likely that aldehydes can react to form Michael additions with RNA as well as with DNA.

Studies have indicated that RNA is more vulnerable than DNA to oxidation by ROS (Brégeon and Sarasin 2005; Li et al. 2006; Moreira et al. 2008; Nunomura et al. 1999). This may result from the fact that most ROS are formed in mitochondria, and the release of ROS from mitochondria is likely to oxidize RNA species in both the cytoplasm and endoplasmic reticulum compartments of the cell before ROS can reach the nucleus, where DNA is located. In addition, RNA as a single-strand molecule is likely to be more susceptible to damage than the tight double strands of DNA.

Nunomura and colleagues (2017) have described the possible consequences of RNA base oxidation to include ribosomal stalling (decreased rate of full-length peptide formation); synthesis of truncated, nonfunctional peptides; and even synthesis of mutated peptides.

RNA oxidation has generated recent clinical interest because it has been found in the early stages of neurodegenerative disorders, such as Alzheimer disease (Nunomura et al. 2017). Nunomura and colleagues speculate that the high level of oxidized RNA in brain neurons results from continuous exposure to ROS. RNA oxidation has also been associated with diabetes: in some patients, free 8-oxoG can be detected in the urine (Broedbaek et al. 2013, Kjaer et al. 2018).

THE INVESTIGATORS' PRIOR RESEARCH ON RNA OXIDATION

As the current study was getting underway, Contreras and colleagues (Baldridge et al. 2015) reported the effects of exposure of a human alveolar lung cell line, A549, to a mixture of acrolein, methacrolein, and ozone at concentrations similar to those used in the current study, using the same in vitro exposure system (described in the Methods section below). They reported that a 1-hour exposure to a mixture of 872 ppb acrolein, 698 ppb methacrolein, and 4 ppm ozone resulted in an approximately 50% increase in intracellular 8-oxoG. Neither ozone alone nor the combination of acrolein plus methacrolein increased 8-oxoG levels.

In the current study, Contreras and colleagues used a similar VOC–ozone mixture to expose another human lung cell line, BEAS-2B. The investigators used multitargeted approaches, including transcriptome analysis, cell biology, and biochemistry to compare and extend the findings of Baldridge and colleagues (2015). They aimed to provide a more precise identification of the products at the RNA level and a follow-up at the protein and lipid level.

APPROACH

SPECIFIC AIMS

The goal of the study was to determine how exposure of the human lung cell line BEAS-2B to a specific mixture of acrolein, methacrolein, and ozone (the "VOC–ozone mixture") changed levels of mRNAs and affected the oxidation status of specific mRNAs. The investigators also wanted to evaluate whether transcripts that were oxidized after exposure to the VOC–ozone mixture had an effect on cellular pathways.

Specifically, the investigators proposed to determine:

Aim 1: To determine the effects of an acute dose of a VOC–ozone mixture on the status of RNAs in the human lung cell line BEAS-2B. The investigators addressed this aim by identifying transcripts that were either up- or down-regulated or oxidized, and by quantifying changes in transcript levels after a 90-minute exposure of the lung cell line to the VOC–ozone mixture.

Aim 2: To determine whether the VOC–ozone mixture had potentially adverse effects on cellular pathways that were mediated via oxidation of RNA. For this aim, the investigators used bioinformatic approaches to determine which biological pathways inside lung cells exposed to VOC–ozone were primarily associated with transcripts that were either up- or down-regulated, and which biological pathways were primarily associated with transcripts that had been oxidized.

Based on these findings, Contreras and colleagues performed follow-up experiments to determine how oxidation of specific transcripts might affect levels of specific proteins or lipids inside the exposed cells. The investigators focused on possible effects on the organization of the cytoskeleton and cholesterol synthesis and concentrations.

The investigators also conducted additional biological assays: they evaluated cell injury and viability, by measuring concentrations of lactate dehydrogenase (LDH), an enzyme that helps produce energy and is present in almost all tissues in the body. Its levels rise in response to cell damage. As an additional marker of cell viability, the investigators measured adherence of the cultured cells to the membrane on which the cells were grown. They also measured concentrations of total free 8-oxoG in cell lysates after exposure.

In a preliminary experiment, the investigators also evaluated the effects of exposure to 1 ppm formaldehyde on the organization of the cell's cytoskeleton. They did this in an attempt to provide support for the idea that exposure to the VOC–ozone mixture was not killing the cells (i.e., was not cytotoxic).

METHODS

Generation and Characterization of Exposure Atmosphere

The investigators generated the air pollutant mixture in a dark, temperature-controlled atmospheric reaction chamber. They injected reactants to achieve initial concentrations of 790 ppb acrolein, 670 ppb methacrolein, and 4 ppm ozone, which were mixed together for 10 minutes in the chamber at 37°C and > 35% relative humidity before starting the cell exposure. Reagent concentrations then decayed over time as the reactions proceeded. Subsequently, the aged VOC–ozone mixture was introduced into a module containing the cells to be exposed at a rate of 1.5 liters per minute combined with 0.08 liters per minute carbon dioxide.

The investigators measured the concentrations of gases remaining in the atmospheric chamber and of the particles formed in the reaction. Particle size distribution was measured by a scanning electrical mobility spectrometer, and particle chemical composition was measured by an aerosol chemical speciation monitor. The composition of gas-phase compounds was monitored by time-of-flight chemical ionization mass spectrometry. Generating exposure atmospheres and measuring the composition were done in collaboration with Dr. Lea Hildebrandt Ruiz of the University of Texas, Austin.

Cell Culture and Exposure

Contreras and colleagues used an air–liquid interface system to expose cells of the human lung epithelial cell line BEAS-2B to the VOC–ozone mixture or clean air as a control. In this system, cells were grown on a collagen-coated membrane inserted in a 6-well culture plate, with cell culture medium below the growing cells. During experiments, either the VOC–ozone mixture or clean air was then passed over the top (apical surface) of the cells for 90 minutes. Clean air had fewer than 10 particles per cm^3 and less than 5 ppb gas-phase impurities; CO_2 concentrations were 5% by volume.

The investigators assessed the effects of exposure to the VOC–ozone mixture or clean air either in the cells themselves after lysing them or in the cell culture medium (below the cells' basolateral surface). Effects were assessed either immediately after the exposure ended or several hours later.

Preparation and Identification of RNA Transcripts

Immediately after exposing cells to the VOC–ozone mixture or clean air for 90 minutes, the investigators prepared RNA from lysates of cells adherent to the membrane insert. Purified RNA was then depleted of DNA with the enzyme DNase I. Half the RNA sample from each experimental condition was left untreated, and the other half was depleted of ribosomal RNA, followed by mixing with a monoclonal antibody specific for 8-oxoG. This precipitated out complexes of antibody bound to 8-oxoG-modified RNAs. RNA was freed from the complexes by mixing it with 8-OH-dG nucleosides.

Contreras's colleagues in the Genomic Sequencing and Analysis Facility at the University of Texas, Austin, then prepared and sequenced RNA from both the "nonenriched" pool (the total pool of transcripts in either exposed or control cells) and what they referred to as either "8-oxoG-enriched" or "significantly oxidized" transcripts (transcripts in either exposed or control cells that bound to the 8-oxoG-specific antibody). RNA sequences were then compared with sequences in the Ensembl annotated database (Hubbard et al. 2002) to identify which genes the RNA sequences affected by exposure were derived from.

Transcriptome and Statistical Analysis

Contreras and colleagues focused their analysis on three sets of transcripts that were affected by exposure: those that were upregulated, those that were downregulated, and those that were significantly oxidized or 8-oxoG-enriched.

The investigators used the software package RNA-Seq by Expectation Maximization to estimate transcript abundance from RNA-Seq data (Li and Dewey 2011). They also used DESeq2 (an R package) to estimate differential expression of transcripts. For transcripts that were significantly differentially expressed by exposure alone, they used a P value < 0.05 and a fold change of more than +2 (for upregulated transcripts) or less than −2 (for downregulated transcripts). For oxidized transcripts, they used a P value < 0.05 and a fold change of more than +2 as significantly differentially expressed.

In their biological assays, the investigators presented data as mean plus or minus the standard deviation of triplicate or duplicate samples, and significance was determined by the Student t-test. A P value < 0.05 was considered significant.

Enrichment Analysis

The investigators generated the list of transcripts for enrichment analysis by first selecting only transcripts with adjusted P value < 0.05 and a fold change of more than 2 for upregulated genes and a fold change less than 0.5 for downregulated genes. For the enrichment analysis of oxidized transcripts, they selected only those with adjusted P value < 0.05 and a fold change of more than 2.

The investigators used the Enrichr web tool to generate the top enriched 10 pathways for transcripts upregulated or downregulated by exposure, and for oxidized transcripts. The tool combines enriched terms from the Kyoto Encyclopedia of Genes and Genomes and the WikiPathways and Panther databases, ranking them by a combined score (Chen et al. 2013, Kuleshov et al. 2016).

The investigators performed a similar analysis to generate a combined ranking of the top 10 Gene Ontology terms (Ashburner et al. 2000) to identify biological processes, cellular components, and molecular functions associated with the up- and downregulated transcripts and with oxidized transcripts.

Changes in Cytoskeleton and Cholesterol

To assess potential effects on the cytoskeleton, the investigators preserved the cells with formaldehyde after exposure to the VOC–ozone mixture and then added a solution of phalloidin to specifically stain F-actin filaments. The intracellular pattern and area of actin staining were then assessed by confocal microscopy at different times after the end of the exposure.

For comparison, Contreras and colleagues also evaluated the actin cytoskeleton 6 hours after exposing cells for 2 hours to 1 ppm formaldehyde. They did this to evaluate effects on the cytoskeleton of what they considered a noncytotoxic pollutant exposure.

To assess changes in cholesterol metabolism, the investigators assessed levels of the enzyme farnesyl-diphosphate farnesyltransferase 1 (FDFT1), which is involved in cholesterol synthesis. After exposing cells to the VOC–ozone mixture or clean air, they used western blotting with a monoclonal anti-FDFT1 antibody to assess levels of FDFT1 in cell lysates. Intracellular cholesterol was assessed fluorometrically in cell lysates after exposure.

Cell Injury and Viability

LDH Levels LDH accumulating in the culture medium under the cells was used as a marker of cell injury and assessed by two methods: (a) colorimetrically by measuring levels of enzymatic activity and (b) by liquid chromatography tandem mass spectrometry (LC-MS/MS). The latter method is considered the gold standard assay and was used to address the possibility that the LDH activity determined colorimetrically may have underestimated the extent of cell death as a result of inactivation of LDH by the exposure mixture. The LC-MS/MS assay also allowed an estimate of the two major isoforms of LDH, A and B, found in the cells.

Cell Adhesion Adherence to the membrane insert is a useful marker of cell viability in this system. Lack of adherence to the membrane is considered a measure of cell death. The number of cells adherent to the membrane insert was measured by confocal microscopy at different times for up to 20 hours after the 90-minute exposure.

Levels of 8-oxoG in RNA

Contreras and colleagues measured 8-oxoG in total RNA of DNA-digested cell lysates by ELISA. They indicated that they corrected for free levels of 8-oxoG in RNA metabolism using the factor 0.38.

SUMMARY OF MAIN RESULTS

CHARACTERIZATION OF THE VOC–OZONE MIXTURE AND REACTION PRODUCTS

After aging the VOC–ozone mixture for 10 minutes, the investigators estimated that concentrations of acrolein and methacrolein in the atmospheric chamber decreased by

20%; that is, the concentrations after 10 minutes were about 630 ppb for acrolein and 540 ppb for methacrolein in the mixture that was passed across the surface of the cells. The investigators also estimated that 80% of the ozone was lost between the mixing chamber and the exposure module, resulting in an unreacted starting concentration of approximately 800 ppb ozone in the exposure mixture.

The reactions of ozone with acrolein and methacrolein produced concentrations of secondary organic aerosol of 32.3 μg/m^3 particles. The organic aerosol consisted predominantly of fine (aerodynamic diameter less than or equal to 2.5 μm) and ultrafine (aerodynamic diameter less than or equal to 0.1 μm) particles.

Critique Figure 1 shows that several oxidized products in the reactants had higher numbers of carbon atoms than the starting reactants acrolein and methacrolein, which have three and four carbon atoms, respectively. This indicated that carbon–carbon addition had occurred.

CHANGES IN RNA TRANSCRIPTOME AND PATHWAYS

Critique Figure 2 shows the changes in upregulated, downregulated, and oxidized gene transcripts in BEAS-2B cells after a 90-minute exposure to the VOC–ozone mixture: 153 transcripts were upregulated, and 113 were downregulated.

Analyzing the oxidized transcripts, the investigators found several in the cells exposed to the VOC–ozone mixture, but a few were also identified in the control cells. To focus on oxidized transcripts that were preferentially expressed in the mixture-exposed cells, the investigators defined a further category of transcripts as "8-oxoG-enriched upon exposure"; that is, these transcripts reacted with the anti-8-oxoG antibody and showed increased expression in the exposed compared with control cells — specifically, in which the fold-change ratio for exposed compared with control cells was more than 1.5. Critique Figure 2 shows 222 transcripts fell in this category, meaning they were 8-oxoG-enriched after exposure and showed increased expression in exposed compared with control cells.

Critique Figure 2 also shows that 8 transcripts fell into an overlapping set of 8-oxoG-enriched upon exposure and downregulated transcripts; that is, exposure to the VOC–ozone mixture resulted in a set of 8 oxidized transcripts that were all downregulated compared with control cells**.** One of the 8 oxidized and downregulated transcripts was FDFT1.

CHANGES IN PATHWAYS AND BIOLOGICAL PROCESSES AFFECTED BY EXPOSURE TO THE VOC–OZONE MIXTURE

The investigators found that the following pathways and biological processes were among the top 10 Enrichr pathways and Gene Ontology terms for differentially expressed transcripts (i.e., comparing expression in exposed versus control cells).

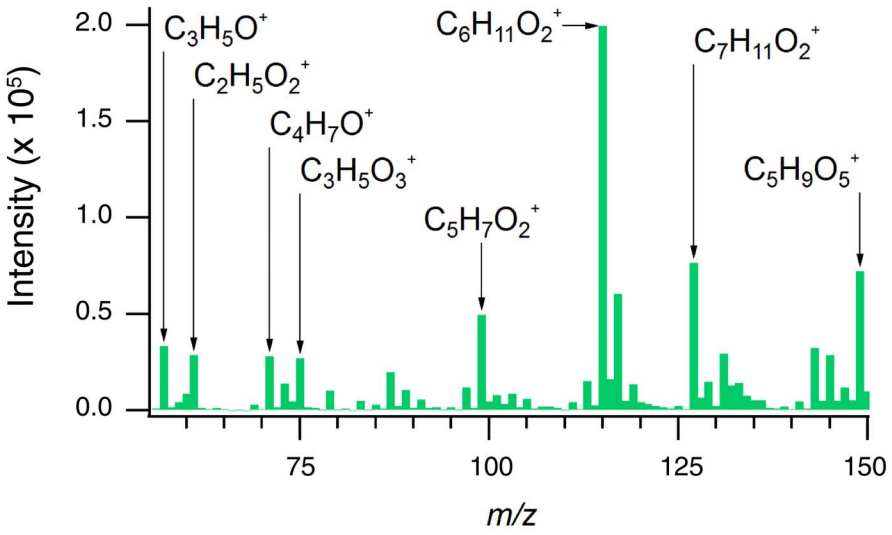

Critique Figure 1. Gas-phase composition of the VOC–ozone mixture observed during the exposure period using chemical ionization mass spectrometry. (From Figure 2 in the Investigators' Report.)

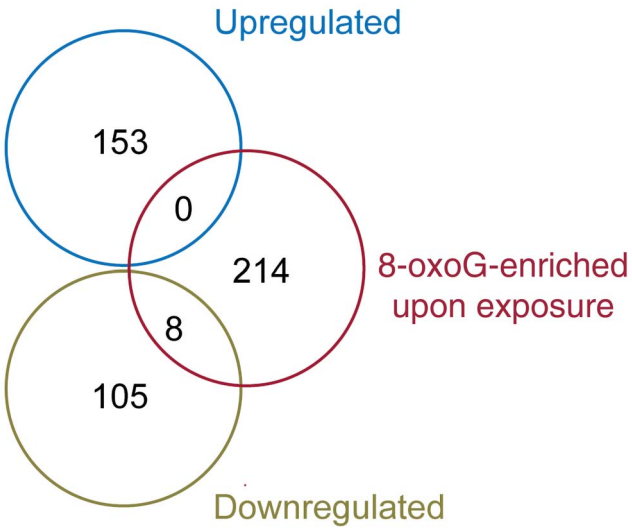

Critique Figure 2. Number of transcripts upregulated, downregulated, or 8-oxoG-enriched after 90-minute exposure of BEAS-2B cells to the VOC–ozone mixture. Eight transcripts were both downregulated and 8-oxoG-enriched upon exposure. (From Figure 4A in the Investigators' Report.)

Upregulated

- *Pathways:* integrin signaling, nanoparticle-mediated signaling, and oncostatin M signaling
- *Gene Ontology terms:* cadherin binding and endoplasmic reticulum lumen

Downregulated

- *Pathways:* apoptosis and adipogenesis
- *Gene Ontology terms:* negative regulation of cell proliferation

Oxidized

- *Pathways:* apoptosis, first apoptotic signal, stress induction of heat shock protein regulation, and epithelial growth factor receptor signaling
- *Gene Ontology terms:* RNA binding, regulation of translation, and RNA metabolic process

BIOLOGICAL MARKERS OF CELL INJURY AND VIABILITY

Exposure of BEAS-2B cells to the VOC–ozone mixture for 90 minutes enhanced cell injury and death as measured by LDH concentrations both by colorimetric and LC-MS/MS assays. Critique Figure 3 indicates a seven-fold increase of LDH concentrations in the culture medium of VOC–ozone-exposed cells compared with control cells, as measured by colorimetry. The LC-MS/MS assay found significant concentrations of both isoforms of LDH in the culture medium of cells exposed to VOC–ozone but none in the medium from control cells.

In addition, exposure to the VOC–ozone mixture decreased the number of cells adherent to the membrane insert. By 20 hours after the exposure only about 30% remained adherent, compared with more than 80% in the control. This result also suggested that exposure to the VOC–ozone mixture was cytotoxic.

FOLLOW-UP BIOLOGICAL ASSAYS

Actin Cytoskeleton

The investigators' preliminary analysis (not shown) found that a pathway identified as actin cytoskeleton was one of the top 10 pathways affected by oxidation of transcripts. However, this result was not replicated in the later analysis shown in the final report. Nonetheless, based on their preliminary findings, the investigators evaluated the effects of exposure on the cytoskeleton.

Ninety-minute exposure to the VOC–ozone mixture changed the organization of actin fibers evaluated 1.5, 7.5, and 20 hours after the end of the exposure. As early as 1.5 hours after the end of the exposure, actin fibers became less organized, were twisted, and formed bright globules of phalloidin stain. The investigators interpreted these findings as disintegration and aggregation of the actin fibers. Exposure to the VOC–ozone mixture also decreased the area of actin by approximately 60% in the cells 20 hours after the end of the exposure. The investigators also indicated that they detected similar changes in the cytoskeleton 6 hours after a 2-hour exposure to 1 ppm formaldehyde.

Lipid Pathway Biosynthesis

Because the transcript of FDFT1, an enzyme involved in lipid biosynthesis, was one of the eight transcripts both significantly oxidized and downregulated by exposure, the investigators evaluated the effects of exposure on two aspects of lipid biosynthesis: the concentrations of FDFT1 protein and of total cholesterol.

At the end of the 90-minute exposure to the VOC–ozone mix, concentrations of FDFT1 protein in BEAS-2B cells were reduced 60% compared with control, and levels of total cholesterol by about 30% compared with control.

Concentrations of Free 8-oxoG

Exposure to the VOC–ozone mixture for 90 minutes increased concentrations of free 8-oxoG approximately 60% within exposed cells compared with control.

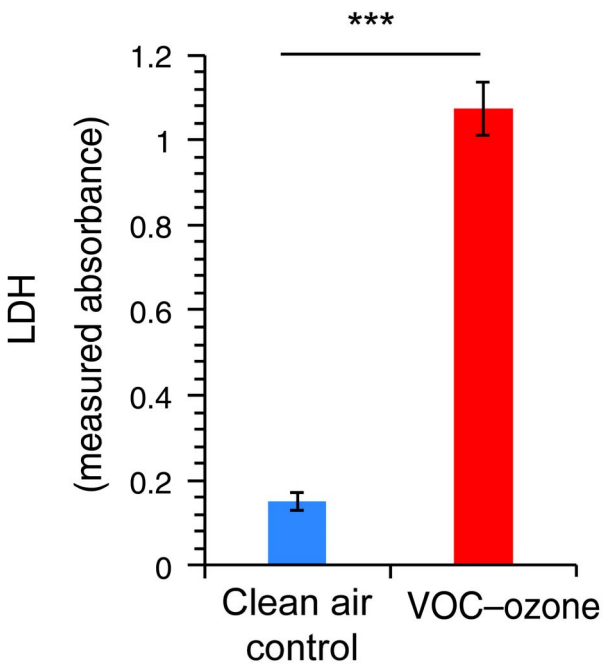

Critique Figure 3. LDH concentrations based on enzymatic activity measured colorimetrically in the culture medium of BEAS-2B cells after exposure to the VOC–ozone mixture or clean air. *** indicates *P* value < 0.0005 using *t*-test. (From Figure 3A in the Investigators' Report.)

REVIEW COMMITTEE EVALUATION

OVERALL COMMENTS

Contreras and colleagues reported many changes in concentrations of specific RNA transcripts after exposure to the VOC–mixture, with more than 150 upregulated, more than 100 downregulated, and more than 200 8-oxoG-enriched. These transcripts were associated with changes in various intracellular pathways, defined by Enrichr and Gene Ontology analyses. The investigators also found changes in the cytoskeleton and cholesterol concentrations in exposed cells. However, they also reported large increases in LDH and loss of cell adherence, both indicators of cell injury and cell death, indicating that the VOC–ozone mixture was toxic to the cells.

The Review Committee considered Contreras and colleagues' work to be an interesting and exciting new approach to the toxicology of air pollution. The study was an important early attempt to gain an understanding of an understudied area: the role of mRNA regulation, modification, and oxidation in the effects of exposure to air pollutants. The investigators used a logical combination of powerful approaches — including cell biology, biochemistry, and transcriptome analysis — to identify candidate genes and pathways for further evaluation of the effects of exposure to pollutants.

The Committee also thought that the use of a mixture of gases — ozone plus the VOCs acrolein and methacrolein — that can combine to produce secondary organic aerosols was potentially relevant to reactants that may be found in some urban atmospheres. The investigators' physicochemical characterization of the particles produced by premixing VOCs and ozone was state of the art. In addition, the investigators used an air–liquid interface in vitro system that is more physiologically representative than many other in vitro methods. This is because lung epithelial cells are exposed to the pollutant gas mixture at the surface of cells grown on membrane inserts suspended in cell culture medium rather than at the bottom of cell culture dishes with lung cells completely immersed in the culture medium.

The Committee also noted that the investigators conducted a logical follow-up of their transcriptome studies by evaluating changes in the protein and lipid concentrations in selected transcripts that had shown changes in expression. These follow-up experiments suggested that changes at the transcript level may indeed have an impact beyond effects on RNA.

However, the Committee noted several important limitations in the study design, as discussed below, which reduced confidence in the ability to generalize the results beyond the current study. Consequently, the Committee considered this study to be an important first step in evaluating the effects of air pollutants on RNA oxidation. This study suggests how the approaches taken may be applied to more exact studies in the future.

DAMAGE CAUSED BY THE EXPOSURE MIXTURE

Based on two key results, the Committee concluded that the exposure mixture damaged or killed the cells exposed to the VOC–ozone mixture. First, many cells that were adherent to the membrane insert at the beginning of the exposure became non-adherent after the 90-minute exposure to the pollutant mixture: 20 hours after exposure only 30% of the cells were still adherent, compared with over 80% in the control population.

Second, concentrations of LDH — a marker of cell injury and death — increased greatly immediately after the 90-minute exposure to the pollutant mixture. The gold standard assay for LDH, LC-MS/MS, showed high concentrations of LDH in the culture medium of cells exposed to the VOC–ozone but negligible concentrations in the culture

medium of control cells. A colorimetric assay also showed large increases in LDH concentrations in the medium of cells exposed to the VOC–ozone mixture (Critique Figure 2). Although the investigators argued that in a previous study a similar seven-fold increase in LDH concentrations was not cytotoxic (Rager et al. 2011), the Committee considered that the combination of the loss of cell adherence to the membrane insert and the large increase in LDH concentrations produced by the pollutant-exposed cells were strong suggestions of the cytotoxic effects of the mixture.

The investigators also argued that the VOC–ozone effects on the cytoskeleton were comparable to the effects of exposure to formaldehyde, which were not cytotoxic, as judged by a similar release of LDH in exposed and control cells. However, the Committee considered that the comparability of these effects on the cytoskeleton was difficult to judge. In addition, the investigators did not provide any evidence for the effects of formaldehyde on cellular adherence or changes in gene transcription, so the Committee could not conclude from the limited evidence provided whether or not exposure to formaldehyde was cytotoxic.

For these reasons, the Committee concluded that some or all of the changes in gene expression and the transcriptome analysis after exposure to VOC–ozone may have been related to the induction of cytotoxicity rather than reflecting a specific response to the pollutant mixture used in the study.

LACK OF RELEVANCE OF HIGH CONCENTRATIONS OF POLLUTANT GASES TO EVERYDAY EXPOSURES

In the current study, the investigators selected starting concentrations of the pollutant gas mixture that were very similar to those they had used in their previous study (Baldridge et al. 2015). Although this allowed some comparison with the results of the previous study, these starting concentrations were very high, and well above concentrations of these pollutants found in everyday urban environments. For example, the investigators estimated that cells were exposed to about 550 ppb acrolein. It is not clear how the investigators arrived at this estimate. But accepting it, this is more than five-fold higher than the permissible exposure level set by the U.S. Occupational Safety and Health Administration (100 ppb) for occupational settings.

Similarly, the investigators estimated that 80% of the ozone was lost before the gas reached the exposure chamber. It was not clear how the investigators estimated this loss. However, if this estimate is accepted, the starting concentration of ozone in the exposure mixture was approximately 800 ppb. This too is a very high concentration of ozone and likely to be cytotoxic to these lung cells.

In their previous study to examine the effects of the same pollutant mix on A549 cells (a different lung cell line derived from a carcinoma) (Baldridge et al. 2015), Contreras and colleagues found small increases in 8-oxoG levels only at these very high concentrations of pollutants. Indeed, based on their previous work, the investigators anticipated that in the current study "exposure conditions were expected to overwhelm cellular defenses." Thus, the Committee considered that the artificially high gaseous concentrations in the exposure protocol in the current study made the findings of uncertain relevance to everyday urban exposures. Future research should consider exposing the cells to more realistic concentrations of gaseous pollutants.

EVALUATION OF TRANSCRIPTOME EFFECTS UNDER LIMITED SETS OF CONDITIONS

Contreras and colleagues evaluated effects of the exposure on RNA transcript levels at only one concentration of pollutant mixture and one time point (i.e., after 90 minutes of exposure). This single time point then provided the basis for the entire Enrichr pathway and gene ontology term analyses. At this time point, the VOC–ozone mixture induced large increases in LDH, which the Committee considered strong evidence of cytotoxicity. The Committee concluded that lower, non-cytotoxic concentrations of the pollutant mixture, evaluated at various time points, might affect genes and pathways in ways that are different from those observed in the current study.

NARROW FOCUS ON 8-oxoG

The Committee recognized that the residual ozone and reactions of the VOCs with ozone would induce RNA oxidation in the cells and result in the formation of 8-oxoG. However, they considered that the narrow focus of the study on a single oxidized RNA product was not well justified. The availability of a specific monoclonal antibody that recognizes 8-oxoG-modified RNA has greatly facilitated the identification of 8-oxoG-modified transcripts in cells. Some previous studies have shown that 8-oxoG may be a relevant marker of disease development in neurological conditions such as Alzheimer disease (Nunomura et al. 2017) and in diabetes (Liu et al. 2016; Kjaer et al. 2018).

However, even at the artificially high exposure levels of VOC and ozone used in the current study, 8-oxoG concentrations inside cells increased by only about 60% after a 90-minute exposure, and Contreras and colleagues found similar, small exposure-related changes in 8-oxoG concentrations in their previous study of a different lung cell line (Baldridge et al. 2015). Thus, the justification for focusing on 8-oxoG as a marker of RNA oxidation in cells exposed

to lower, more "normal" levels of airborne pollutants seems unclear.

Furthermore, even at the transcript level, there is little evidence from the current study to suggest that 8-oxoG is biologically relevant to pollutant exposure in this system. For example, there was little overlap between transcripts that were oxidized and transcripts that were up- or downregulated by exposure. Only eight overlapping transcripts were identified, and all were downregulated. If 8-oxoG were a marker of downregulation after pollutant exposure, one would expect many more transcripts in the overlapping set of transcripts.

Rather, the Committee thought that the way to explore oxidized RNA products in the future would be to identify all products via a more sensitive technique such as LC-MS/MS instead of by using an antibody specific for a single oxidation product. This approach would help to identify RNA oxidation products that were potentially more biologically relevant in this system. The Committee also noted that, as shown in Critique Figure 1, the reactive aldehydes used in this study, acrolein and methacrolein, were likely to form higher-molecular-weight Michael-addition adducts with RNA. This type of RNA product may also be worth exploring in future studies.

OTHER TECHNICAL ISSUES

The Committee noted several other key points of study design that warranted further investigation in future experiments.

Cell Culture Conditions

The investigators showed that clean-air-exposed control cells contained several oxidized transcripts. They speculated that these oxidized transcripts reflected a basal level of cellular oxidation in the absence of environmental stress. However, the Committee considered that the BEAS-2B cells — derived from normal bronchial cells — may indeed have been undergoing oxidative stress by being grown at atmospheric oxygen concentrations (around 21%; or 149 mmHg partial pressure) instead of the lower oxygen concentrations (around 13%; or 109 mmHg) found in the alveolar environment in the lung. Kumar and colleagues (2016) have indicated that at atmospheric oxygen tension, lung cells grown in vitro have blunted responses to external stimuli such as nanoparticles compared with the responses when the cells are exposed at the lower oxygen tension found in the lung. Thus, future studies of RNA oxidation should consider culturing lung cells under these lower, more physiologically appropriate oxygen tensions.

Potential for Artifactual Oxidation of RNA

Although the investigators were careful in their extraction of RNA from the cells, the Committee considered that the level of oxidized RNA detected might have been modified by the extraction procedure. Thus, the true level of oxidized RNA in the cell may be different from what was reported. The Committee noted that this artifactual oxidation during extraction — referred to as "side oxidation" — was a major problem in early studies of DNA oxidation (e.g., Cadet et al. 2002; Hamilton et al. 2001; Nakae et al. 1995; Ravanat et al. 2002). Consequently, estimates of oxidized DNA varied widely. Fewer studies have looked at this issue in the field of RNA oxidation. Thus, more studies with different extraction methods are needed to show consistent concentrations of oxidized RNA in lung cells as well as other cell types.

SUMMARY AND CONCLUSIONS

The Committee considered Contreras and colleagues' work an interesting and exciting new approach to the toxicology of air pollution. The study was an important initial attempt to gain an understanding of an understudied area, namely, the role of mRNA regulation, modification, and oxidation in the effects of exposure to air pollutants. The investigators used a logical combination of powerful approaches — including cell biology, biochemistry, and transcriptome analysis — to identify candidate genes and pathways for further evaluation of the effects of exposure to pollutants.

Exposing cells to a mixture of gases — ozone plus the VOCs acrolein and methacrolein — that can combine to produce secondary organic aerosol particles was potentially relevant to assessing the effects of reactants that may be found in some urban atmospheres. Contreras and colleagues' physicochemical characterization of the particles produced by pre-mixing the gaseous components was also state of the art. They used an air–liquid interface in vitro system that is more physiologically representative than many in vitro methods because cells are directly exposed to the pollutant gas mixture instead of mixing pollutants into the culture medium.

However, the Committee noted several important limitations in the study design that reduced confidence in the generalizability of the results toward understanding the role of RNA oxidation after exposure to air pollution. One major limitation was that the concentrations of VOCs and ozone that Contreras and colleagues used to expose the cells in the current study appeared to be cytotoxic and were much higher than would be found even in heavily

polluted urban environments. Given the use of a single mixture, at one high exposure level, and measured at only one time point, the biological relevance of the identified RNA oxidation products was not clear.

In addition, the Committee noted that Contreras and colleagues focused on a single RNA oxidation product, 8-oxoG. This focus was understandable given the availability of a specific monoclonal antibody that recognized this molecule, but it was not well justified from a theoretical perspective. In future studies, other potentially more biologically relevant RNA oxidation products need to be identified using more sensitive techniques. Other technical issues such as the possibility that the cell cultures were conducted at too high an oxygen level and uncertainty over the true level of oxidized RNA in the cells raised questions about the broader usefulness of the results obtained.

Nonetheless, the Committee considered the report to be an important preliminary demonstration of RNA oxidation in lung cells exposed to a VOC–ozone mixture. This powerful combination of techniques — including transcriptome analysis, biochemistry, and cell biology — offers a template to be applied to more exact and comprehensive studies in the future.

ACKNOWLEDGMENTS

The Review Committee thanks the ad hoc reviewers for their help in reviewing the scientific merit of the Investigators' Report. The Committee is also grateful to Annemoon van Erp and Geoffrey Sunshine for their oversight of the study and assistance in preparing its Critique, to George Simonson for his editing of the Investigators' Report and Critique, and to Hope Green, Fred Howe, Hilary Selby Polk, and Ruth Shaw for their roles in preparing this Research Report for publication.

REFERENCES

Ashburner M, Ball CA, Blake JA, Botstein D, Butler H, Cherry JM, et al. 2000. Gene ontology: Tool for the unification of biology. The Gene Ontology Consortium. Nat Genet 25(1):25–29.

Baldridge KC, Zavala J, Surratt J, Sexton KG, Contreras LM. 2015. Cellular RNA is chemically modified by exposure to air pollution mixtures. Inhal Toxicol 27:74–82.

Brégeon D, Sarasin A. 2005. Hypothetical role of RNA damage avoidance in preventing human disease. Mutat. Res 577: 293–302.

Broedbaek K, Siersma V, Henriksen T, Weimann A, Petersen M, Andersen JT, et al. 2013. Association between urinary markers of nucleic acid oxidation and mortality in type 2 diabetes: A population-based cohort study. Diabetes Care 36(3):669–676.

Byvoet P, Balis JU, Shelley SA, Montgomery MR, Barber MJ. 1995. Detection of hydroxyl radicals upon interaction of ozone with aqueous media or extracellular surfactant: The role of trace iron. Arch Biochem Biophys 319:464–469.

Cadet J, Douki T, Frelon S, Sauvaigo S, Pouget JP, Ravanat JL. 2002. Assessment of oxidative base damage to isolated and cellular DNA by HPLC-MS/MS measurement. Free Radic Biol Med 33:441–449.

Cataldo F. 2006. Ozone degradation of biological macromolecules: Proteins, hemoglobin, RNA, and DNA. Ozone Sci Eng 28:317–328.

Chen EY, Tan CM, Kou Y, Duan Q, Wang Z, Meirelles GV, et al. 2013. Enrichr: Interactive and collaborative HTML5 gene list enrichment analysis tool. BMC Bioinformatics 128.

Cooke MS, Olinski R, Loft S; European Standards Committee on Urinary (DNA) Lesion Analysis. 2008. Measurement and meaning of oxidatively modified DNA lesions in urine. Cancer Epidemiol Biomarkers Prev 17:3–14.

Hallquist M, Wenger JC, Baltensperger U, Rudich Y, Simpson D, Claeys M, et al. 2009. The formation, properties and impact of secondary organic aerosol: Current and emerging issues. Atmos Chem Phys 9:5155–5236.

Hamilton ML, Guo Z, Fuller C, Van Remmen H, Ward WF, Austad SN, et al. 2001. A reliable assessment of 8-oxo-2-deoxyguanosine levels in nuclear and mitochondrial DNA using the sodium iodide method to isolate DNA. Nucleic Acids Res 29:2117–2126.

Hubbard T, Barker D, Birney E, Cameron G, Chen Y, Clark L et al. 2002 The Ensembl genome database project. Nucleic Acids Res 30:38–41.

Kelly FJ. 2003 Oxidative stress: Its role in air pollution and adverse health effects. Occup Environ Med 60:612-616.

Kjaer LK, Oellgaard J, Henriksen T, Gaede P, Pedersen O, Poulsen HE. 2018. Indicator of RNA oxidation in urine for the prediction of mortality in patients with type 2 diabetes and microalbuminuria: A post-hoc analysis of the Steno-2 trial. Free Radic Biol Med 129:247–255.

Kroll JH, Seinfeld JH. 2008. Chemistry of secondary organic aerosol: Formation and evolution of low-volatility organics in the atmosphere. Atmos Environ 42:3593–3624.

Kuleshov MV, Jones MR, Rouillard AD, Fernandez NF, Duan Q, Wang Z, et al. 2016. Enrichr: A comprehensive gene set enrichment analysis web server 2016 update. Nucleic Acids Research 44 (W1):W90–97.

Kumar A, Dailey LA, Swedrowska M, Siow R, Mann GE, Vizcay-Barrena G, et al. 2016. Quantifying the magnitude of the oxygen artefact inherent in culturing airway cells under atmospheric oxygen versus physiological levels. FEBS Lett.590:258-269.

Li B, Dewey CN. 2011. RSEM: Accurate transcript quantification from RNA-Seq data with or without a reference genome. BMC Bioinformatics. 12:323.

Li N, Hao M, Phalen RF, Hinds WC, Nel AE. 2003. Particulate air pollutants and asthma. A paradigm for the role of oxidative stress in PM-induced adverse health effects. Clin Immunol 109(3):250–265.

Li Z, Wu J, Deleo CJ. 2006. RNA damage and surveillance under oxidative stress. IUBMB Life 58:581–588.

Liu X, Gan W, Zou Y, Yang B, Su Z, Deng J, et al. 2016. Elevated levels of urinary markers of oxidative DNA and RNA damage in type 2 diabetes with complications. Oxid Med Cell Longev 1-7.

Moreira PI, Nunomura A, Nakamura M, Takeda A, Shenk JC, Aliev G, et al. 2008. Nucleic acid oxidation in Alzheimer disease. Free Radic Biol Med 44:1493–1505.

Nakae D, Mizumoto Y, Kobayashi E, Noguchi O, Konishi Y. 1995. Improved genomic/nuclear DNA extraction for 8-hydroxydeoxyguanosine analysis of small amounts of rat liver tissue. Cancer Lett 97:233–239.

Nunomura A, Lee HG, Zhu X, Perry G. 2017. Consequences of RNA oxidation on protein synthesis rate and fidelity: Implications for the pathophysiology of neuropsychiatric disorders. Biochem Soc Trans 45:1053–1066.

Nunomura A, Perry G, Pappolla MA, Wade R, Hirai K, Chiba S, et al. 1999. RNA oxidation is a prominent feature of vulnerable neurons in Alzheimer's disease. J Neurosci 19:1959–1964.

Rager JE, Smeester L, Jaspers I, Sexton KG, Fry RC. 2011. Epigenetic changes induced by air toxics: Formaldeyde exposure alters mRNA expression in human lung cells. Environ Health Persp 119:494–500.

Ravanat JL, Douki T, Duez P, Gremaud E, Herbert K, Hofer T, et al. 2002. Cellular background level of 8-oxo-7,8-dihydro-2′-deoxyguanosine: An isotope based method to evaluate artefactual oxidation of DNA during its extraction and subsequent work-up. Carcinogenesis. 23:1911–1918.

Stevens JF, Maier CS. 2008. Acrolein: Sources, metabolism, and biomolecular interactions relevant to human health and disease. Mol Nutr Food Res 52:7–25.

U.S. EPA (U.S. Environmental Protection Agency). 2013. Integrated Science Assessment (ISA) of Ozone and Related Photochemical Oxidants (Final Report, Feb 2013). EPA/600/R-10/076F. Washington, DC: U.S. EPA.

RELATED HEI PUBLICATIONS: OZONE AND AIR TOXICS

Number	Title	Principal Investigator	Date
Research Reports			
198	Understanding the Health Effects of Isoprene-Derived Particulate Matter Enhanced by Anthropogenic Pollutants	J.D. Surratt	2019
197	Composition and Oxidative Properties of Particulate Matter Mixtures: Effects of Particle Phase State, Acidity, and Transition Metals	N.L. Ng	2019
192	Multicenter Ozone Study in oldEr Subjects (MOSES)		
	Part 1. Effects of Exposure to Low Concentrations of Ozone on Respiratory and Cardiovascular Outcomes	M.W. Frampton, J.R. Balmes, P. A. Bromberg, P. Stark	2017
	Part 2. Effects of Personal and Ambient Concentrations of Oxone and Other Pollutants on Cardiovascular and Pulmonary Function	D.Q. Rich and M. W. Frampton	2020
191	Protective Role of Eosinophils and Tumor Necrosis Factor-α after Ozone Inhalation	A.D. Fryer	2017
155	The Impact of the Congestion Charging Scheme on Air Quality in London		
	Part 2. Analysis of the Oxidative Potential of Particulate Matter	F. Kelly	2011
150	Mutagenicity of Stereochemical Configurations of 1,3-Butadiene Epoxy Metabolites in Human Cells	R.Q. Meng	2010
149	Development and Application of a Sensitive Method to Determine Concentrations of Acrolein and Other Carbonyls in Ambient Air	T.M. Cahill	2010
147	Atmospheric Transformation of Diesel Emissions	B. Zielinska	2010
146	The Role of T Cells in the Regulation of Acrolein-Induced Pulmonary Inflammation and Epithelial-Cell Pathology	M.T. Borchers	2009
125	Uptake Distribution of Ozone in Human Lungs: Intersubject Variability in Physiologic Response	J.S. Ultman	2004
109	Ozone-Induced Modulation of Airway Hyperresponsiveness in Guinea Pigs	R.B. Schlesinger	2002
106	Effects of Combined Ozone and Air Pollution Particle Exposure in Mice	L. Kobzik	2001
90	Aldehydes (Nonanal and Hexanal) in Rat and Human Bronchoalveolar Lavage Fluid After Ozone Exposure	M.W. Frampton	1999
85	Mechanisms of Response to Ozone Exposure: The Role of Mast Cells in Mice	S.R. Kleeberger	1999
Special Report			
16	Mobile-Source Air Toxics: A Critical Review of the Literature on Exposure and Health Effects	HEI Air Toxics Review Panel	2007

Copies of these reports can be obtained from HEI; PDFs are available for free downloading at www.healtheffects.org/publications.

ABBREVIATIONS AND OTHER TERMS

8-OH-dG	8-hydroxy-2′-deoxyguanosine nucleoside
8-oxoG	8-oxo-7,8-dihydroguanine
A549	adenocarcinomic human alveolar basal epithelial cell line
ACR	acrolein
ACSM	aerosol chemical speciation monitor
ALI	air–liquid interface
ATP	adenosine triphosphate
BEAS-2B	bronchial epithelial lung cell line
BEGM	bronchial epithelial cell growth medium
CIMS	chemical ionization mass spectrometer
COPD	chronic obstructive pulmonary disease
DMA	differential mobility analyzer
DNA	deoxyribonucleic acid
EGFR	epithelial growth factor receptor
ELISA	enzyme-linked immunosorbent assay
FC	fold change
FAS	first apoptotic signal
FDFT1	farnesyl-diphosphate farnesyltransferase 1 (squalene synthase)
GAPDH	glyceraldehyde 3-phosphate dehydrogenase
GO	gene ontology
HPLC	high-performance liquid chromatography
KEGG	Kyoto Encyclopedia of Genes and Genomes
LDH	lactate dehydrogenase
LC-MS/MS	liquid chromatography tandem mass spectrometry
LPM	liters per minute
MACR	methacrolein
miRNA	microRNA
mRNA	messenger RNA
NO_x	nitrogen oxides
PBS	phosphate buffer solution
PM	particulate matter
$PM_{2.5}$	particulate matter $\leq$ 2.5 μm in aerodynamic diameter
RFA	request for applications
RH	relative humidity
RNA	ribonucleic acid
ROS	reactive oxygen species
rRNA	ribosomal RNA
SDS	sodium dodecyl sulfate
SEMS	scanning electrical mobility system
VOC	volatile organic compound

HEI BOARD, COMMITTEES, and STAFF

Board of Directors

Richard F. Celeste, Chair *President Emeritus, Colorado College*

Enriqueta Bond *President Emerita, Burroughs Wellcome Fund*

Jo Ivey Boufford *President, International Society for Urban Health*

Homer Boushey *Emeritus Professor of Medicine, University of California, San Francisco*

Michael T. Clegg *Professor of Biological Sciences, University of California, Irvine*

Jared L. Cohon *President Emeritus and Professor, Civil and Environmental Engineering and Engineering and Public Policy, Carnegie Mellon University*

Stephen Corman *President, Corman Enterprises*

Martha J. Crawford *Dean, Jack Welch College of Business and Technology, Sacred Heart University*

Michael J. Klag *Dean Emeritus and Second Century Distinguished Professor, Johns Hopkins Bloomberg School of Public Health*

Alan I. Leshner *CEO Emeritus, American Association for the Advancement of Science*

Henry Schacht *Managing Director, Warburg Pincus; Former Chairman and Chief Executive Officer, Lucent Technologies*

Research Committee

David A. Savitz, Chair *Professor of Epidemiology, School of Public Health, and Professor of Obstetrics and Gynecology, Alpert Medical School, Brown University*

Jeffrey R. Brook *Senior Research Scientist, Air Quality Research Division, Environment Canada, and Assistant Professor, University of Toronto, Canada*

Francesca Dominici *Professor of Biostatistics and Senior Associate Dean for Research, Harvard T.H. Chan School of Public Health*

David E. Foster *Phil and Jean Myers Professor Emeritus, Department of Mechanical Engineering, Engine Research Center, University of Wisconsin, Madison*

Amy H. Herring *Sara & Charles Ayres Professor of Statistical Science and Global Health, Duke University, Durham, North Carolina*

Barbara Hoffmann *Professor of Environmental Epidemiology, Institute of Occupational, Social, and Environmental Medicine, University of Düsseldorf, Germany*

Allen L. Robinson *Raymond J. Lane Distinguished Professor and Head, Department of Mechanical Engineering, and Professor, Department of Engineering and Public Policy, Carnegie Mellon University*

Ivan Rusyn *Professor, Department of Veterinary Integrative Biosciences, Texas A&M University*

Review Committee

James A. Merchant, Chair *Professor and Founding Dean Emeritus, College of Public Health, University of Iowa*

Kiros Berhane *Professor and Chair, Department of Biostatistics, Mailman School of Public Health, Columbia University*

Michael Jerrett *Professor and Chair, Department of Environmental Health Sciences, Fielding School of Public Health, University of California, Los Angeles*

Frank Kelly *Professor of Environmental Health and Director of the Environmental Research Group, King's College London*

Jana B. Milford *Professor, Department of Mechanical Engineering and Environmental Engineering Program, University of Colorado, Boulder*

Jennifer L. Peel *Professor of Epidemiology, Colorado School of Public Health and Department of Environmental and Radiological Health Sciences, Colorado State University*

Roger D. Peng *Professor of Biostatistics, Johns Hopkins Bloomberg School of Public Health*

HEI BOARD, COMMITTEES, and STAFF

Officers and Staff

Daniel S. Greenbaum *President*
Robert M. O'Keefe *Vice President*
Rashid Shaikh *Director of Science*
Jacqueline C. Rutledge *Director of Finance and Administration*
Emily Alden *Corporate Secretary*

Lee Ann Adelsheim *Research Assistant*
Hanna Boogaard *Consulting Principal Scientist*
Sofia Chang-DePuy *Digital Communications Manager*
Aaron J. Cohen *Consulting Principal Scientist*
Robert M. Davidson *Staff Accountant*
Philip J. DeMarco *Compliance Manager*
Hope Green *Editorial Project Manager*
Joanna Keel *Research Assistant*
Lissa McBurney *Science Administrative Assistant*
Janet I. McGovern *Executive Assistant*
Pallavi Pant *Staff Scientist*
Allison P. Patton *Staff Scientist*
Hilary Selby Polk *Managing Editor*
Anna S. Rosofsky *Staff Scientist*
Robert A. Shavers *Operations Manager*
Annemoon M.M. van Erp *Managing Scientist*
Eleanne van Vliet *Staff Scientist*
Donna J. Vorhees *Director of Energy Research*
Katherine Walker *Principal Scientist*

HEALTH
EFFECTS
INSTITUTE

75 Federal Street, Suite 1400
Boston, MA 02110, USA
+1-617-488-2300
www.healtheffects.org

RESEARCH
REPORT

Number 201
July 2020